

5-4-2011

# Residual Strength of Ultra-High Performance Concrete After Exposure to Elevated Temperatures

Brian T. Burke
burkeb1@gmail.com

# Residual Strength of Ultra-High Performance Concrete after Exposure to Elevated Temperatures

Brian T. Burke

B.S., Southern Connecticut State University, 2008

A Thesis

Submitted in Partial Fulfillment of the

Requirements for the Degree of

Master of Science

at the

University of Connecticut

2011

APPROVAL PAGE

Master of Science Thesis

# Residual Strength of Ultra-High Performance Concrete After Exposure to Elevated Temperatures

Presented by

Brian Thomas Burke, B.S.

Major Advisor _____
Michael Accorsi

Associate Advisor _____
Adam Zofka

Associate Advisor _____
Ramesh Malla

University of Connecticut

2011

# Acknowledgements

I would like to express my sincere gratitude to my advisor Prof. Michael Accorsi for the continuous support of my study and research. His guidance helped me in all aspects of my graduate study.

Besides my advisor, I would like to thank the rest of my thesis committee: Prof. Adam Zofka and Prof. Ramesh Malla for their encouragement, insightful comments, and hard questions.

I thank my parents, Tom and Betty Burke, for their enduring support during my collegiate journey. I also would like to thank my grandfather, Gregory Sgroi, for beginning my engineering education when I still learning to walk.

Last, but not least, I would like to thank my wife, Tiffany. Without her inspiration and patience I would never have earned my masters.

# Table of Contents

# Chapter 1 - A Review of Ultra-High Performance Fiber-Reinforced Concrete


## Abstract

Ultra-high performance concrete (UHPC) represents the latest advancements in concrete technology. The material characteristics of UHPC are significantly greater than the current concretes classified as high-performance concretes (HPC).These traits are made possible through advances in particle packing models, increased quality control of materials and the introduction of various types of fibers. The increased strength of UHPC has implications on the current testing methods. In addition, the increased packing density of UHPC introduces explosive spalling when exposed to elevated temperatures. This paper attempts to introduce the principles the allow UHPC to achieve compressive strengths exceeding 29 ksi (200 MPa) and discuss the implications that this has on testing the material. A discussion of the material and thermal properties of UHPC, as they relate to explosive spalling, is also included.


## 1.1 Introduction

Ultra-high performance concrete (UHPC) reflects the latest advancements in concrete technology. UHPC is a fiber-reinforced concrete (FRC) that has significantly improved properties of strength, toughness and durability. UHPC is typically very dense, has very-high compressive strength and a water-cementitious material ratio (*w/cm*) below 0.2. The workability properties are attained through optimization of the ‘granular packing’ and the use of high-range

water-reducing admixtures. The addition of steel fibers increases the ductility and tensile strength of UHPC. The cement is a Portland cement with a high content of silica (HTS Lafarge). Sand and silica flour are quartz grade of 300 and 5 microns size. The silica fume (SF) is a low alkali and carbon content one. The superplasticizer is a PEG-based (OPTIMA 100, Chryso).

### 1.1.1 High-Performance Concrete

UHPC falls in the larger category of high-performance concretes (HPC). Normal strength concrete (NSC) and HPC contain the same principle ingredients of cement, water and aggregate. High-performance concretes were first made commercially available in the early 1980s in the form of high-strength concretes (HSC). Their development over the next few decades proceeded rather slowly and this lead to several different definitions for HPC. For example, the American Concrete Institute (ACI) provides the following definition for HPC “concrete meeting special combinations of performance and uniformity requirements that cannot always be achieved routinely using conventional constituents and normal mixing, placing, and curing practices [1]” This definition does not require any one special property, but rather a combination of properties. The Portland Cement Association of America (PCA) takes a similar approach and considers concretes with characteristics optimized for specific applications and environments. The PCA lists the following desirable characteristics for HPCs [2]:

> High strength, high early strength, high modulus of elasticity, high abrasion resistance, high durability and long life in severe environments, low permeability and diffusion, resistance to chemical attack, high resistance to frost and deicer scaling damage, toughness and impact resistance, volume stability, ease of placement, compaction without segregation and inhibition of bacterial and mold growth.

Given the PCA's and ACI's criteria, a normal strength concrete designed for ease of placement and resistance to chemical attack would also considered a HPC, therefore high strength is not a requirement for high performance concrete.

The apparent vagueness of these definitions is due to the fact that many of the characteristics of high-performance concretes are interrelated [1]. Therefore, if several characteristics are desired it may be at the expense of some other characteristics. An additional definition suggests that HPC's exhibit high-workability, high-strength and high durability [3]. The criteria provided by Mehta, allows for an easy distinction between HPC and ultra-high-performance concrete (UHPC). For a more complete definition of UHPC it has been said that UHPC is an HPC with a compressive strength over 150 MPa (22000 psi), tensile strengths over 8 MPa (1200 psi) and exhibit strain-hardening behavior under uniaxial tension [4].

## 1.2 Development and Material Characterization

### 1.2.1 High-Strength Concrete (HSC)

The classification of a concrete as high-strength is based largely in part on the compressive strength of concretes found in normal practice. The definition of high-strength concrete (HSC) has changed over the last few decades. These changes reflect advancements in mix design, quality control, chemical admixtures and materials. In the 1960's a mix design that called for a compressive strength over 35 MPa (5000 psi) was considered an HSC [5]. Compressive strengths of concrete had not improved much by the 1980s. A

concrete mix that exhibited compressive strengths greater than 40 MPa (6000 psi) would be considered an HSC [3]. ACI gives high-strength concrete a minimum compressive strength design value of 55MPa (8000psi). In the same report, the authors show how the definition of HSC can vary based on geographical location [6]. Today, PCA considers HSC as concretes with compressive strengths over 70 MPa (10,000 psi) [2].

High-strength concretes typically get their high compressive strength from material selection and quality control. The cement is chosen based on its long-term compressive strength. The principal strength-producing compounds in cement are the calcium silicates. The hydration of calcium silicates is represented in shorthand notation by:

$$\mathbf{C_3S + H \rightarrow C\text{-}S\text{-}H + CH}$$

Where **$C_3S$** is calcium silicate, **H** is water, **C-S-H** is calcium silicates hydrate and **CH** is calcium hydroxide.

Mineral admixtures such as silica fume, fly ash and blast furnace slags can be blended with the cement or used as a partial replacement for fine aggregates [2, 7]. The mineral admixtures react with the calcium hydroxide, which is a byproduct of the hydration process of Portland cement.

$$\mathbf{Pozzolan + CH + H \rightarrow C\text{-}S\text{-}H}$$

This pozzolanic reaction provides several benefits. It is a slow reaction, which reduces the rate of heat liberation and strength development. The reaction increases the overall strength of the cement by replacing the strength-reducing

calcium hydroxide with additional calcium silicate hydrates. In addition, the reaction products fill up the capillary spaces, which improve the strength and impermeability of the cement paste [3, 7].

### 1.2.2 Packing Density

The concept of packing density is a fundamental principle in the design of high-performance concretes [8]. Much of the work on packing density was performed in the 1970's and 1980's by researchers in France [9, 10] and Denmark [Bache]. In the design of ultra-high performance concrete mixes, this concept is applied to the cementitious materials. Increasing the particle packing density is analogous to reducing the capillary porosity of the hardened cement. The capillary porosity controls the strength and permeability of the hardened paste [7]. As the capillary porosity decreases, the compressive strength increases [12]. Particles with grain sizes smaller than cement, such as silica fume, can act as fillers in the cement paste matrix, thereby reducing the water requirements and increasing the strength of the concrete [7]. A two-dimensional representation of this packing effect can be seen in Fig. 1-1. A scanning electron microscope image of the granular packing for both UHPC and normal strength concrete is shown in Fig. 1-2. Several models exist to predict the particle packing density of the cementitious materials [10, 13]. These models are based on the particle size distribution and specific packing density values and can be used to optimize the packing density [9]. Laboratory efforts to maximize the packing density of the cementitious materials has resulted in water-to-cementitious material (*w/cm*) ratio as low as 0.14 [10] and compressive strengths as high as 800 MPa (116,000 psi) [14].

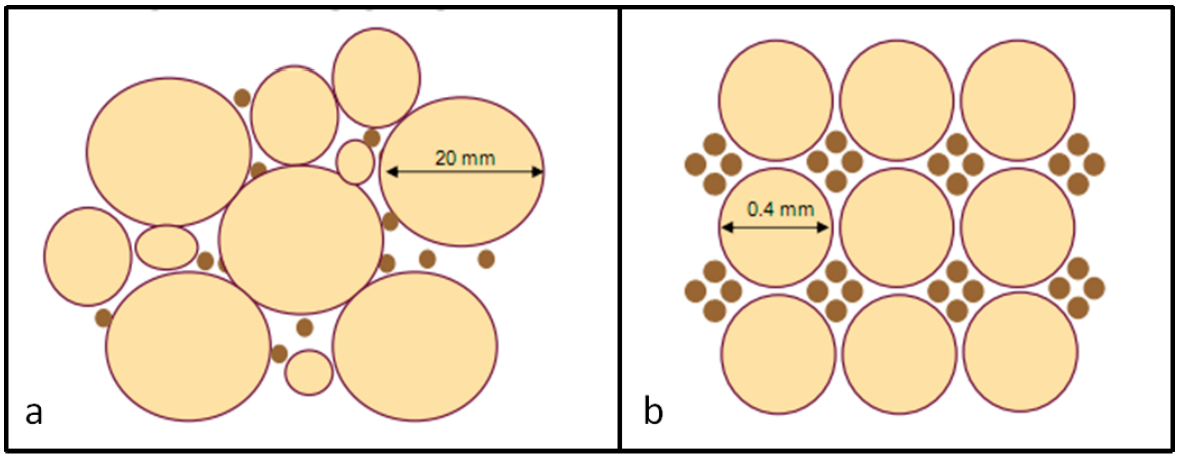


**Figure 1-1. Two-dimensional schematic comparison particle packing of normal strength concrete (a) and UHPC (b). [15].**

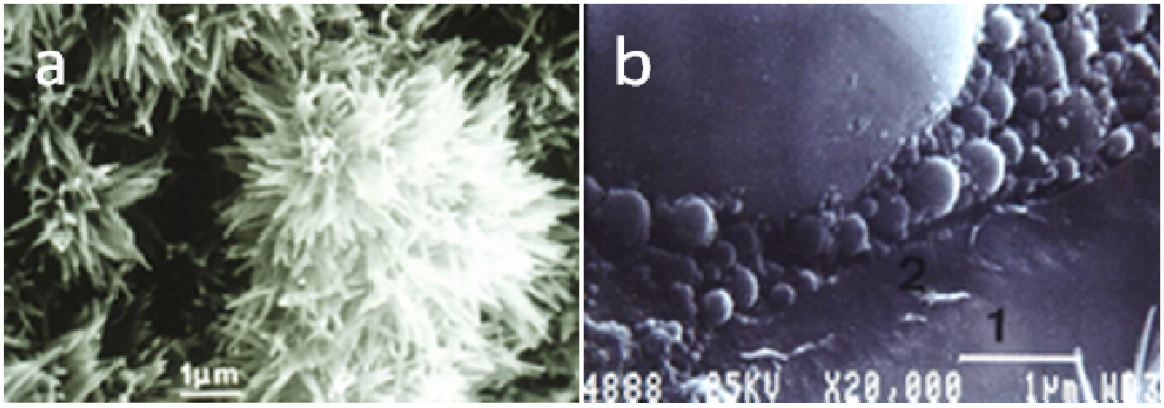


**Figure 1-2. Scanning electron microscope images of cement hydrates of NSC (a) and granular packing of UHPC. [16].**

### 1.2.3 Reactive Powder Concrete (RPC)

Reactive powder concretes reflect further refinements of the mixture proportioning and curing conditions. The elimination of the coarse aggregate allows for an improved homogeneity of the mixture. High-range water reducing admixtures (HWRA) are used to increase the ability of the ultra-fine particles to fill the void spaces. The use of super-plasticizers further reduces the need for water in the mixture. Optimization of the granular mixture and the application of

pressure during the curing process increases the packing density. Pressure applied during the curing process eliminates entrapped air and most of the chemical contraction that accompanies the hydration reactions [17]. Exposure to heat treatment after setting enhances the microstructure. The addition of steel fibers achieves increased ductility and tensile strength [14]. The resulting mixture is essentially made of powders and steel fibers [17].

### 1.2.4 Fiber Reinforced Concrete (FRC)

Fiber-reinforced concrete contains hydraulic cement, water, aggregate and discontinuous discrete fibers [3]. The use of fibers to strengthen brittle materials is not a new concept. Straw and horsehair have been added to clay to form bricks for millennia [18]. Steel is the most common type of fiber, but they can also be made from glass, plastic and natural materials. The fibers may come in various shapes, sizes and quantities. UHPC can be classified into three different classes based on fiber size and the fiber volume fraction (Table 1-1). UHPCs that contain fibers are also referred to as ultra-high performance fiber-reinforced concrete (UHPFRC).

The addition of steel fibers to ultra-high performance concrete increases the tensile strength and ductility. The function of the fibers in producing these properties depends on their size, percent volume of mix and bond with the cement matrix. Short fibers control the opening and propagation of microcracks. On the structural scale this equates to an increased tensile strength. Long fibers control the larger cracks that appear in the concrete at higher loads. This produces a strain-hardening effect as the concrete continues to carry load

beyond its initial cracking. The effects of the different size fibers are shown in Fig. 1-3. If the steel fibers do not have a sufficient bond with the cement matrix and they slip out at low loads, none of these benefits will be realized.

**Table 1-1. Classification of UHPC by fiber content. Adapted from [19]**

| Classification | Fiber Content, % by volume | Fiber Length | Properties |
|---|---|---|---|
| **Type 1** | 5 – 10 | <6 mm (0.24in.) | • Increased tensile strength<br>• Little impact on ductility<br>• Requires high percentage of traditional reinforcing bars |
| **Type 2** | 2 – 3 | 13 – 20mm (0.51 – 0.79in.) | • Increased tensile strength<br>• Increased ductility<br>• Requires minimal traditional reinforcing bars |
| **Type 3** | <11 | 1 – 20mm (0.04 – 0.79 in.) | • Significantly increased tensile strength<br>• Significantly increased ductility<br>• Does not require any traditional reinforcing bars |

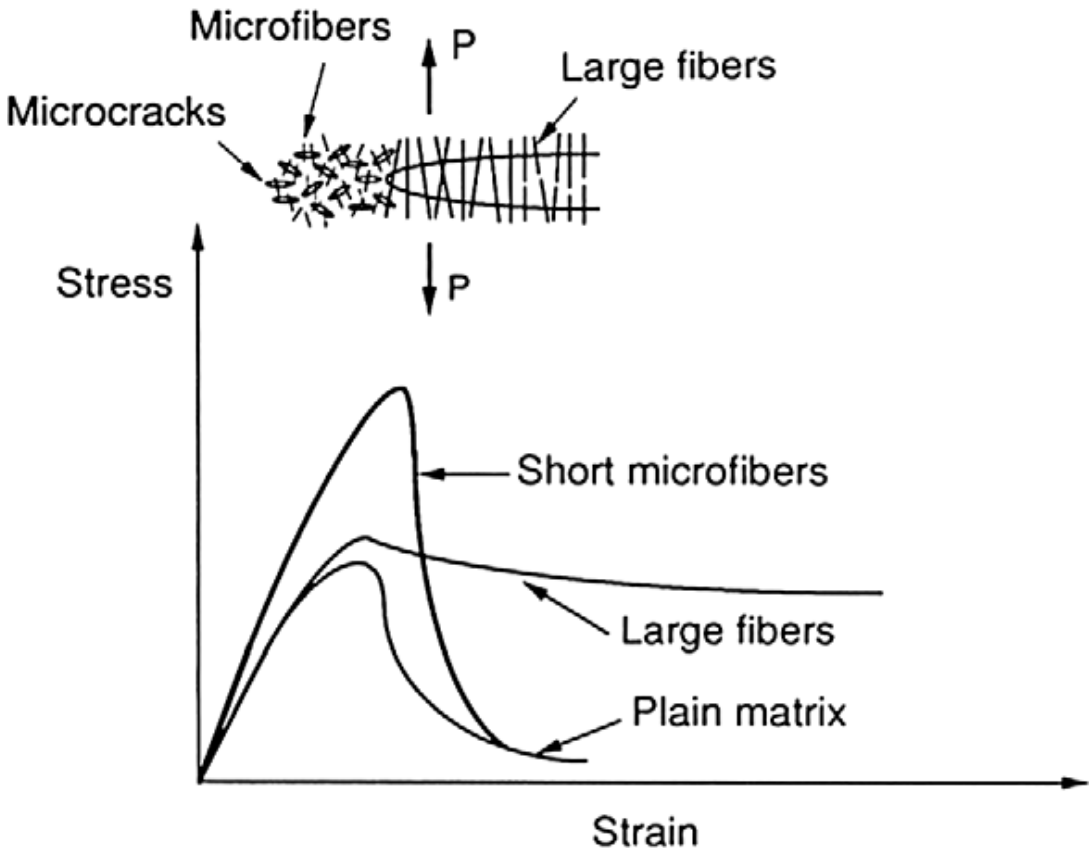


**Figure 1-3. Impact of relative fiber size on stress-strain curve of FRC [3].**

The orientation of the fibers has a significant impact on the tensile strength. The higher percentage of fibers that are parallel to the tensile force, the greater their contribution to the tensile strength. Since the casting method mould shape of a specimen plays a significant role in the orientation of the fibers, the tensile strengths of differently shaped specimens made from the same fiber-reinforced concrete can vary greatly [19].

## 1.3 Material Characterization

### 1.3.1 General

In 2002 the Association Française de Génie Civil (AFGC) produced *Ultra-High-Performance Fiber-Reinforced Concretes – Interim Recommendations.* This document was the first reference on the use of UHPFRCs in civil engineering. The Federal Highway Administration (FHWA) published a report [20] that "characterizes the material behaviors of one UHPC in terms of accepted concrete testing methodologies." This report, the first of its kind on UHPC in the US, endeavored to evaluate a commercially available UHPC (Ductal-FM®) as a potential material in highway bridges. The research focused on ASTM and AASHTO standard testing procedures. The standard testing procedures were modified as needed and new tests were developed when necessary. Over one thousand individual specimens were tested.

The study primarily examined 51, 76 and 102mm (2, 3 and 4 in.) cylinders as well as 51 and 76 mm (2 and 3 in.) cubes. The researchers considered a 76 mm (3 in.) diameter cylinder as the control specimen. The results of the compressive properties of this ultra-high performance concrete are summarized in Table 1-2.

**Table 1-2. FHWA compressive strength test results. [20]**

| Curing Regimen | Compressive strength, MPa (ksi) | | Modulus of elasticity, GPa (ksi) | | Strain at peak stress | |
|---|---|---|---|---|---|---|
| | Average | Standard deviation | Average | Standard deviation | Average | Standard deviation |
| Steam | 193 (28.0) | 14 (2.0) | 52.7 (7640) | 1.5 (218) | 0.0041 | 0.0004 |
| Untreated | 126 (18.3) | 14 (2.0) | 42.7 (6190) | 1.5 (218) | 0.0035 | 0.0002 |

Graybeal also compared the impact of various casting, curing and testing factors on the reported properties. The specimens were exposed to the manufacturer's recommended curing regimen, an untreated curing regimen, a tempered (lower temperature) steam regimen and a delayed steam regimen. The results of the comparison found that, regardless of the curing regimen, UHPC provided improved performance over NSC and HPC in all properties. Steam-based curing further improved these properties.

## 1.4 Testing - Considerations and Limitations

### 1.4.1 Equipment and Procedures

The high compressive strength of UHPC and other high-strength concretes poses a problem to research facilities and materials testing laboratories. The current testing standards and equipment were developed for concretes with compressive strengths of 10 to 40 MPa (1500 to 6000 psi) and they may not be suited to testing high-strength concretes. A standard 152 mm (6 in.) diameter cylinder with a compressive strength of 200 MPa (29.0 ksi) results in an expected load of 3600 kN (810 kip). High-strength concrete specimens exhibit a large energy release upon failure. This sudden release of energy can affect the measured test result and have detrimental effects on the calibration of the load

frame. To account for the increased stiffness required from the load frame, it has been suggested to use a load frame with a capacity equal to 150% the expected load [21,22]. Continuing the example from before, this leads to a desired load frame capacity of 5400 kN (1200 kip) capacity.

An interlaboratory test program that was designed to evaluate the current ASTM testing standard for concrete as applied to high-strength concretes provided further insight into the effect of the load frame on the test results [23]. Burg showed that the ASTM recommended size of the load frame test platen (spherical bearing blocks), proves to be inadequate at compressive strengths above 70 MPa (10,000 psi). Load frames with inadequate test platen were about 10% lower than those from an adequately equipped machine. The effect of the load platen rigidity further reduces the measured compressive strength of the specimen as the strength of the concrete increases (see Fig. 1-4). [23]

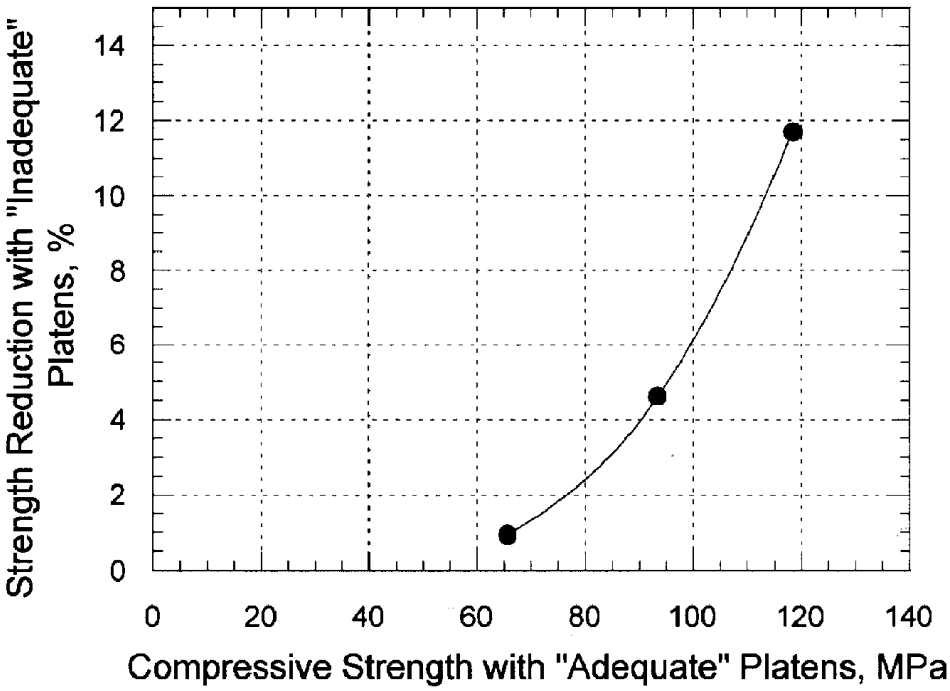


**Figure 1-4. Effect of inadequate platens on results of compressive strength of HSC. [23]**

In North America, the standard specimen is a cylinder. Additional concern when testing UHPC cylinders is their end-conditions. When casting cylinders the fibers and workability of the mix prevent the technician from achieving a 'clean' screeding action on the top of the cylinder. This leaves a test specimen with a very rough surface and possibly out-of-plane test surface. ASTM C39 requires the end surfaces of a cylinder to be plane within 0.05mm (0.002 in). To obtain accurate results, uniform and repeatable load transfer from the load frame to the testing specimens must be achieved [23]. For specimens that have rough and out of plane surfaces ASTM C39 allows the use of capping compounds, unbounded caps or end grinding. These procedures will provide a uniform distribution of load into the test specimens. However, the very-high strength of UHPC precludes the use of capping compounds or unbounded neoprene caps. Generally, capping compounds should be at least equal in strength to the test specimen and neoprene pads should not be used for testing specimens over 90 MPa (13 ksi) [24].The remaining option is to use a cylinder end grinder. Since the installation of cylinder end grinders is cost prohibitive for most laboratories, several different approaches have been developed to overcome this obstacle. These methods are similar in approach to the current cylinder capping procedure for normal strength concretes [21,25]. Both methods rely on increasing the compressive strength of the capping material by confining it with a steel ring or similar apparatus (see Fig. 1-5). These methods have been shown to achieve results comparable to end grinding for concretes with compressive strengths up to 110 MPa (16 ksi).

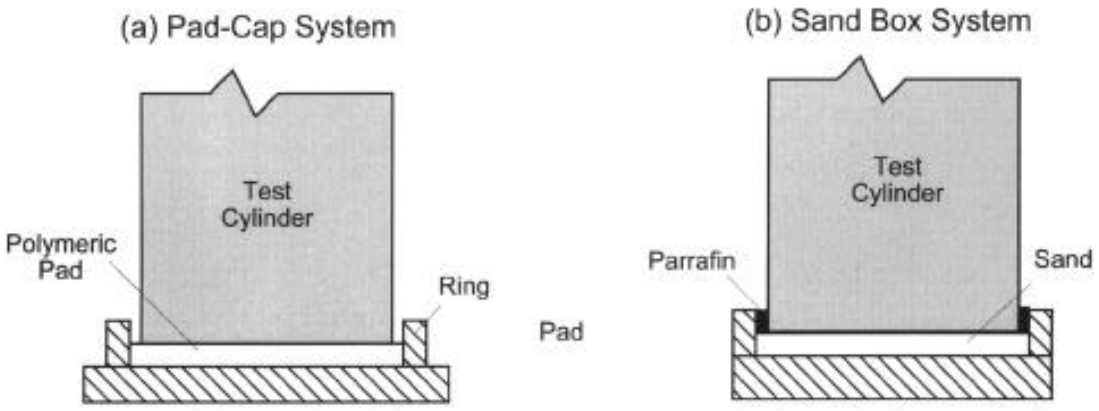


**Figure 1-5. Alternative test specimen capping methods for testing HSC. [26]**

Another approach to solving this issue is to use cube specimens. By its nature, the cube specimen provides two testing surfaces that are plane and free from defect. This is ideal for compression testing. However, the cube shape does not provide the same uniform stress field that develops in cylindrical specimens. Lateral stresses are introduced into compression specimens from friction between the specimen ends and the load platen. The development of the lateral stresses is dependent on the specimen geometry. Cylindrical specimens of adequate height (about twice the diameter) will have a mid-height area that is unaffected by lateral stress, thereby providing uniaxial stress. Cubes are affected by lateral stresses throughout their height and, therefore, are in a state of multi-axial stress (Fig. 1-6) [26]. As a result cube specimens measure a higher compressive strength than cylinders. For normal strength concrete it has been shown that a cylinder can report about 20% less than a cube [27].

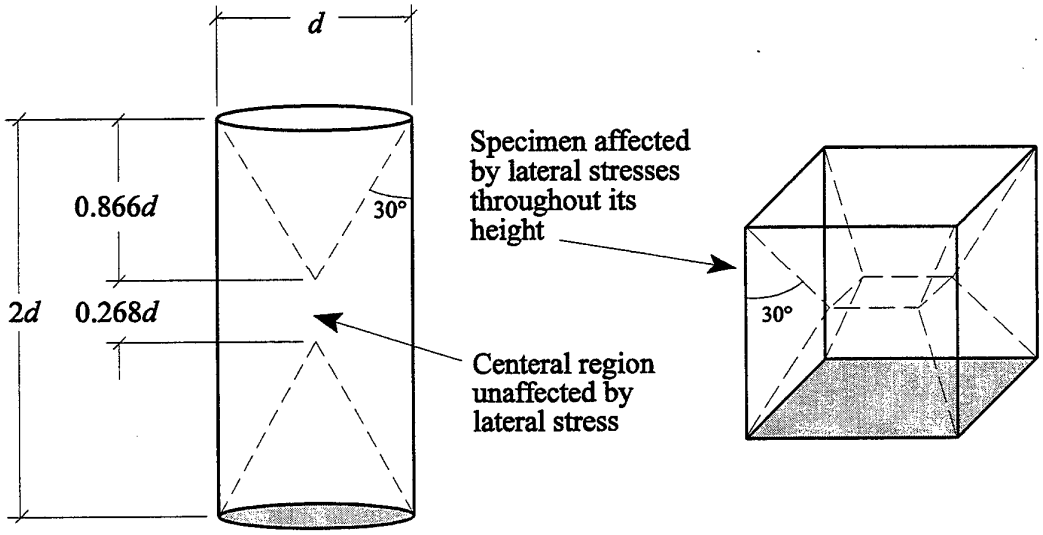


**Figure 1-6. Approximate effects of multiaxial stresses in cylinder and cube specimens. [26]**

Graybeal completed a comprehensive study that compared the effects of specimen shape and size on ultra-high-performance fiber-reinforced concrete with strengths ranging from 80 to 200 MPa (11.6 to 29 ksi). This study determined that the shape accounted for no more than an 8 percent difference. The results of his cylinder-cube comparison study are summarized in Table 1-3. [28]

**Table 1-3. Coefficients for conversion of compressive strength results from specimens of different geometry. Adapted from [28].**

| Shape | Tested | Desired cylinder size | |
|---|---|---|---|
| | | 76 mm (3 in.) | 102 mm (4 in.) |
| Cube | 100 mm (4 in.) | 1.00 | 1.00 |
| | 70.7 mm (2.78 in.) | 0.94 | 0.93 |
| | 51 mm (2.01 in) | 0.96 | 0.96 |
| Cylinder | 102 mm (4.02 in) | 1.01 | -- |
| | 76 mm (3.00 in.) | -- | 0.99 |
| | 51 mm (2.01 in.) | 1.08 | 1.07 |

The steel fiber reinforcement included in UHPC provides a number of advantages, most notably in terms of tensile structural behavior. Normally, a compression test on high-strength concrete would result in a very brittle, dramatic failure. UHPC that is reinforced with steel fibers does not exhibit explosive failures during compression tests. A compression test on steam-treated UHPC would likely result in a rapid load drop, but the cylinder would remain intact.

## 1.5 Tensile Properties

Determining the tensile properties of concrete test specimens has always proven to be a difficult task. Traditional concrete has very little tensile strength and attempts to use a direct tension method, similar to that for testing steel, introduces additional stresses at the grips. These additional stresses either cause a multiaxial stress field which influences the tensile field or cause the specimen to fail at the grips. Two standard tests are used to determine the tensile properties of concrete through indirect means. These tests are the split-cylinder and flexural beam test. The split cylinder test yields the splitting tension strength. The flexural beam results in the modulus of rupture. The modulus of rupture is not a very accurate measure of the tensile strength of concrete because it depends on the assumption that concrete behaves in a linear manner. The flexural beam test is not used in practice for quality control because it is a larger shape. These results are useful to engineers who are designing concrete structures. Expressions for the values can be found in ACI 318. The split-cylinder test provides a more accurate and reliable measure of the tensile properties of concrete. The test is completed with the same size cylinders used for

compression testing and does not require any additional testing apparatus. This no longer holds true when testing fiber-reinforced concretes. The addition of steel fibers adds a new level of complexity to the evaluation of the results. The strain-hardening behavior of fiber-reinforced concretes enables the material to continue to carry load well past the initial cracking and the peak strength may not correspond to the tensile cracking strength [29,30,31]. In order to capture the true tensile cracking strength of ultra-high-performance fiber-reinforced concretes, additional instrumentation is required. The proposed devices utilize LVDT's to measure the transverse deformation of the test specimen as the load is applied. This arrangement allows for the observation of both first cracking as well as post-cracking behaviors [31].

## 1.6 Thermal Properties and Performance

### 1.6.1 Concrete at Elevated Temperatures

Concrete has long been recognized for its superior performance over other building materials at elevated temperatures. It is often the material of choice to provide an additional level of public safety against a fire hazard. In many steel structures, concrete is often used as fire protection. Concrete is incombustible, a good insulator against heat and when exposed to high temperatures it does not release toxic fumes. Additionally, after exposure to elevated temperatures normal strength concrete retains much of its strength and exhibits minimal spalling. This residual strength allows occupants to escape and rescue efforts to continue in a fire damaged structure.

### 1.6.2 Residual Strength

High-strength concretes do not perform as well in high temperature environments. The residual strength of HSCs exposed to temperatures between 100$^{o}$C and 400$^{o}$C (212$^{o}$F and 752$^{o}$F) is as much as 40% of its room temperature strength. This reduction in strength is approximately 20 to 30% more than normal strength concretes [32].

### 1.6.3 Spalling & Pore Pressure

The very high compressive strengths, self-healing and durability characteristics of UHPC arise mainly from its increased packing density. This increased packing density results in an increased susceptibility to explosive spalling due to its reduced porosity. When exposed to elevated temperatures, UHPC exhibits explosive spalling at temperatures below that of normal strength concrete. An explanation of the mechanisms behind explosive spalling in UHPCs is shown in the Fig. 1-7.

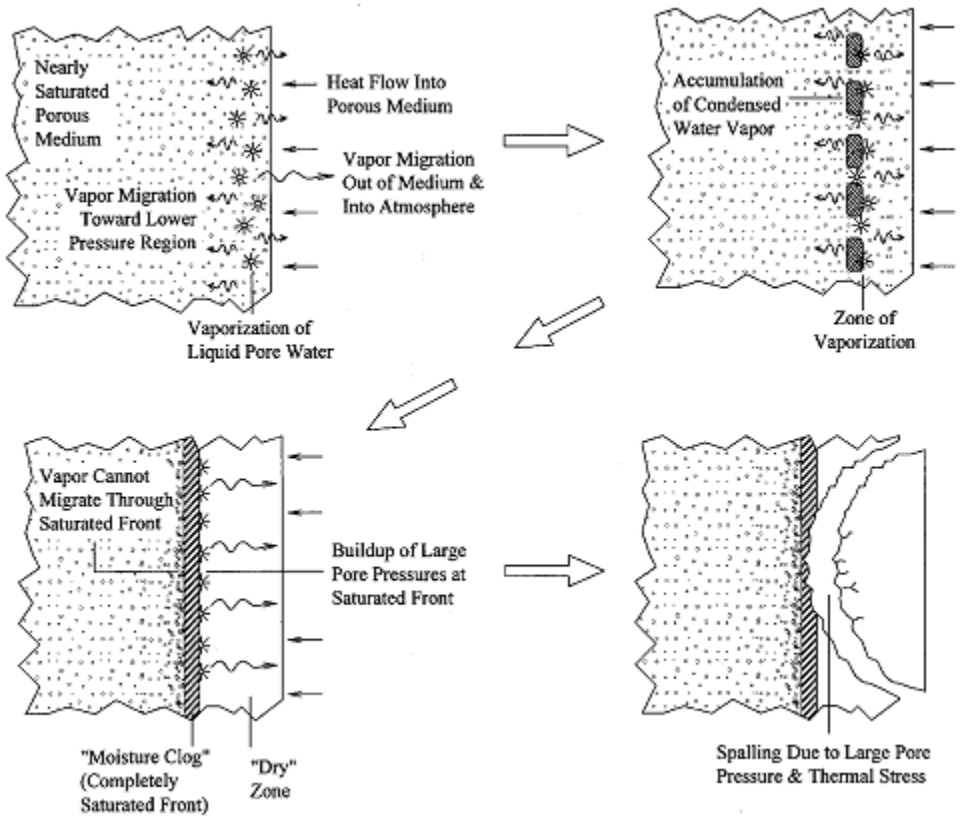


**Figure 1-7. Sequence of step leading to fire induced spalling [33].**

This ‘moisture clog’ phenomenon is the primary mechanism behind explosive spalling due to elevated temperatures [33,34]. As the concrete is heated, the free water vaporizes and migrates through the pore structure. When the water vapor reaches the unsealed surface, it evaporates. As the moisture diffuses inwardly, it comes into contact with cooler concrete and condenses. This condensate will add to the liquid that is already in the pores of this region. This vaporize-migrate-condense cycle will continue until a completely saturated front develops. This front effectively reduces the permeability and prevents the moisture from escaping to the surface. If the porosity of the concrete is low enough, then the vaporized moisture will increase the pore pressure until the tensile strength of the

concrete is reached. At this point the concrete will explosively spall. The permeability of the concrete and the rate of heating are the two factors that determine the existence of a moisture clog. A concrete exposed to a sufficiently high heating rate or one with a very low permeability will explosively spall when internal pore pressures develop that exceed the strength of the concrete.

Thermal diffusivity is a function of the thermal conductivity, specific heat and density of a material. It measures the ability of a material to conduct thermal energy relative to its ability to store energy. The addition of steel fibers to a concrete increases the thermal diffusivity by 50 to 100 % when compared to a standard concrete mix [35]. The addition of steel fibers increases the explosiveness of the spalling. The increased tensile strength of steel fiber reinforced concretes allows the concrete to store more energy that is then released when the concrete spalls [36].

## 1.7 Conclusion

Ultra-high performance concrete represents a new class of concretes. It is the result of several decades of research and development. Its durability, compressive strength and tensile properties make it an ideal material for next generation structures. However, the behavior of this high-performance material under elevated temperatures and when used in fire-resistant applications, warrants further study.

## References


[1] H.G. Russell, ACI defines high-performance concrete, Concrete International. 21 (1999) 56–57.

[2] S.H. Kosmatka, B. Kerkhoff, W.C. Panarese, Design and control of concrete mixtures, 14th ed., Portland Cement Assoiation, Skokie, IL, 2003.

[3] P.K. Mehta, P.J. Monteiro, Concrete: microstructure, properties, and materials, McGraw-Hill, 2006.

[4] K. Habel, M. Viviani, E. Denarié, E. Brühwiler, Development of the mechanical properties of an ultra-high performance fiber reinforced concrete (UHPFRC), Cement and Concrete Research. 36 (2006) 1362-1370.

[5] A.M. Neville, Properties of Concrete., Wiley, New York, 1963.

[6] ACI Committee 363, High-Strength Concrete (ACI 363R), Special Publication. 228 (2005) 79-80.

[7] J.F. Young, S. Mindess, R.J. Gray, A. Bentour, The Science and Technology of Civil Engineering Materials, Prentice Hall, Upper Saddle River, NJ, 1998.

[8] H.H. Wong, A.K. Kwan, Packing density: a key concept for mix design of high performance concrete, in: Proceedings of Materials Science and Technology in Engineering Conference (MaSTEC), Hong Kong, 2005.

[9] F. de Larrard, Ultrafine particles for the making of very high strength concrete, Cement and Concrete Research. 19 (1989) 161-172.

[10] F. de Larrard, Optimization of high-performance concrete, in: Proceedings of the international conference jmx 13 on micromechanics of concrete and cementitious composites, 03/09 - 03/10/93, Publ by Presses Polytechniques Et Universitaires Romandes, Lausanne, Switzerland, 1993: p. 45.

[11] H.H. Bache, Model for strength of brittle materials built up of particles joined at points of contact, Journal of The American Ceramic Society. 53 (1970) 654–658.

[12] T.C. Powers, Structure and physical properties of hardened Portland cement paste, Journal of the American Ceramic Society. 41 (1958) 1-6.

[13] H.H. Wong, A.K. Kwan, Packing density of cementitious materials: Part 1-measurement using a wet packing method, Materials and Structures/Materiaux Et Constructions. 41 (2008) 689-701.

[14] V. Perry, TH17 - Ultra-High Performance Ductile Concrete, CONSTRUCT2009. (2009).

[15] The technology of Ductal® Technology, http://www.ductal-lafarge.com/wps/portal/ductal/6_1-Ductal_overview (2010).

[16] P. Richard, M. Cheyrezy, Composition of reactive powder concretes, Cement and Concrete Research. 25 (1995) 1501–1511.

[17] O. Bonneau, C. Poulin, J. Dugat, P. Richard, P.C. Aitcin, Reactive powder concrete: from theory to practice, Concrete

[18] A.M. Brandt, Fibre reinforced cement-based (FRC) composites after over 40 years of development in building and civil engineering, Composite Structures. 86 (2008) 3-9.

[19] P. Rossi, Ultra-high-performance fiber-reinforced concretes, Concrete International. 23 (2001) 46–52.

[20] B.A. Graybeal, Material Property Characterization of Ultra-High Performance Concrete., (2007).

[21] S.A. Mizra, C.D. Johnson, Compressive strength testing of high performance concrete cylinders using confined caps, Construction and Building Materials. 10 (1996) 589-596.

[22] M. Lessard, O. Challal, P.C. Aticin, Testing high-strength concrete compressive strength, ACI Materials Journal. 90 (1993).

[23] R.G. Burg, M.A. Caldarone, G. Detwiler, D.C. Jansen, T.J. Willems, Compression testing of HSC: latest technology, Concrete International. 21 (1999) 67–76.

[24] M.F. Pistilli, T. Willems, Evaluation of cylinder size and capping method in compression strength testing of concrete, Cement, Concrete and Aggregates. 15 (1993) 59-69.

[25] C. Boulay, F. de Larrard, The Sand-Box A new capping system for testing HPC Cylinders, Concrete International. 15 (1993) 63-66.

[26] D.J. Elwell, G. Fu, Compression testing of concrete: cylinders vs. cubes, New York State Department of Transportation, Transportation Research and Development Board, 1995.

[27] A.M. Neville, Properties of concrete, J. Wiley, New York, 1996.

[28] B.A. Graybeal, M. Davis, Cylinder or cube: strength testing of 80 to 200 Mpa (11.6 to 29 ksi) ultra-high-performance fiber-reinforced concrete, ACI Materials Journal. 105 (2008) 603.

[29] A.E. Naaman, H.W. Reinhardt, Strain hardening and deflection hardening fiber reinforced cement composites, Year: 2003. (2003) 95–113.

[30] A. Nanni, Splitting-tension test for fiber reinforced concrete, ACI Materials Journal. 85 (1988) 229-233.

[31] B.A. Graybeal, Practical means for determination of the tensile behavior of ultra-high performance concrete, Jai. 3 (2006)

[32] L.T. Phan, High-Strength Concrete at High Temperature-An Overview, in: International Symposium on Utilization of High-Strength, High-Performance Concrete, June, 2002: pp. 16–20.

[33] G.R. Consolazio, M.C. McVay, J.W. Rish III, Measurement and prediction of pore pressures in saturated cement mortar subjected to radiant heating, ACI Materials Journal. 95 (1998) 525-536.

[34] X.T. Chen, T. Rougelot, C.A. Davy, W. Chen, F. Agostini, F. Skoczylas, et al., Experimental evidence of a moisture clog effect in cement-based materials under temperature, Cement and Concrete Research. 39 (2009) 1139–1148.

[35] M. Behloul, G. Chanvillard, P. Casanova, G. Orange, F.F.F. France, Fire resistance of Ductal Ultra high Performance Concrete, in: Proc, n.d.: pp. 101-110.

[36] Fédération internationale du béton. Task Group 4.3., Fire design of concrete structures - structural behaviour and assessment: State-of-art report, International Federation for Structural Concrete, Lausanne, Switzerland, 2008.

# Chapter 2 – Current Structural Applications of Ultra-High Performance Concrete


## Abstract

Ultra-high performance concrete (UHPC) exhibits material and structural properties far greater than that of normal strength and even high-performance concrete. This paper provides a brief introduction to the theory behind UHPC. The Mars Hill Bridge in Wapello County, Iowa; the Cat Point Creek Bridge in Richmond, Virginia and the Jakway Park Bridge in Buchanan County, Iowa are among the UHPC bridges discussed in this paper. In addition, the paper highlights some of the obstacles preventing widespread adoption of UHPC as a structural material in the transportation industry.


## 2.1 Introduction

Ultra high performance concrete (UHPC) refers to a class of concretes that take advantage of advances in concrete technology to achieve compressive strengths on the order of 200 MPa (30ksi). While this is the most notable feature when compared to normal strength concretes (NSC) and high strength concretes HSC, it is not the only significant difference. Additional improvements of UHPC over other concretes include ductility, increased durability and lower permeability. It is the combination of these advanced material properties that make UHPC such an impressive product. UHPC has been researched in Europe and Asia for about ten years and, within the last few years; it has made its way to the shores of North America [1,2,3].

### 2.1.1 Theory & Mix Design

Ultra high performance concrete mix designs differ from traditional concrete mix designs in that they contain no coarse aggregate. The UHPC mix relies on achieving optimum particle packing and reactive powders to develop many of its extraordinary features. The basic premise behind particle packing is to increase the density of the concrete and develop a uniform microstructure by filling the voids between the cement particles. This is, in effect, similar to the function of fine aggregates in traditional concretes. The UHPC mix accomplished this by replacing the use of a coarse aggregate with the silica fume. Silica fume is small enough to fit in the voids and it reacts in the concrete mix to produce additional binder materials. Table 2-1 summarizes the differences in mix design [1,3].

**Table 2-1. Components of the UHPC premix. Adapted from Graybeal [1]**

| Material | Quantity [kg/m$^3$ (lb/yd$^3$)] | UHPC [% by weight] | Traditional Concrete Mix [% by weight] |
|---|---|---|---|
| **Coarse Aggregate** | N/A | N/A | 35-50 |
| **Portland Cement*** | 712 (1,200) | 28.5 | 15-25 |
| **Fine Sand*** | 1020 (1,720) | 40.8 | 28-40 |
| **Silica Fume*** | 231 (390) | 9.3 | N/A |
| **Ground Quartz*** | 211 (355) | 8.4 | N/A |
| **Superplasticizer** | 30.7 (51.8) | 1.2 | 0-0.3 |
| **Accelerator** | 30.0 (50.5) | 1.2 | 0-0.1 |
| **Steel Fibers** | 156 (263) | 6.2 | N/A |
| **Water** | 109 (184) | 4.4 | 5-8 |

In addition to the introduction of silica fume, the UHPC mix also relies on fibers to develop some of its characteristics. Usually these are high-strength steel fibers, but they can also be organic fibers. Proper distribution and orientation of the

fibers in the concrete matrix is critical to achieving the increased tensile properties of UHPC. For this reason, it is recommended that any UHPC elements be cast in controlled settings [1].

## 2.2 Structural Applications

Several uses of ultra high performance concrete in structural applications have been demonstrated in the last few years. The first UHPC bridge in North America opened in 2006 in Iowa, a second bridge opened in October 2008 in Virginia and in November 2008 another UHPC bridge opened in Iowa. In addition to these three bridges, UHPC has been used in New York as a joint material between deck bulb-tee girders, and for canopies for a Light-Rail Transit Station and a pedestrian bridge both in Calgary, Canada [3].

Bridges constructed with ultra high performance concrete have already been constructed in France, Japan, Australia and South Korea. The function of these bridges range from a footbridge in Seoul, South Korea to highway overpasses in the Drome Region, France.

### 2.2.1 Mars Hill Bridge

The first UHPC bridge constructed in the United States is the Mars Hill Bridge in Wapello County, Iowa. The bridge is a 110-ft simple span three girder design that replaced an aging steel truss bridge. Without any U.S. specifications for working with UHPC, the designer relied on guidelines that were developed in France. The designer based his design on a standard Iowa State bulb-tee section design. To save material costs, he narrowed the flange and web thicknesses. The final design uses 47 0.6-inch diameter, low-relaxation prestressing strands in the

bottom flange stressed to 72% of ultimate strength. There is no shear reinforcement in the girder. In addition to following the French design specifications, this design was also reviewed by Franz-Josef Ulm of the Massachusetts Institute of Technology. Ulm has done much research on concrete including working with the FHWA to develop prototype UHPC bridge design.

Following completion of the design process, a 71-foot test specimen was cast constructed with identical section properties and strand layout. The main goal of this testing was to verify the release stresses. After losses, the designers estimated a cracking load for the beam between 240 and 280 kips. The test results showed the cracking load to be 256 kips, thus confirming some of their design assumptions. This testing was completed in mid-2005 and by early 2006 the bridge was opened to traffic [4,5].

### 2.2.2 Cat Point Creek Bridge

The second UHPC bridge built in the United States is the Cat Point Creek Bridge in Richmond County, VA. This is a ten-span bridge with ten girders per span, but one of the spans consists of only five UHPC girders. This span is 80 feet and the UHPC girders are the same shape as the conventional-concrete girders. However, the additional tensile strength provided by the steel fibers in the UHPC, allowed the designers to omit the provision for shear reinforcement. The designer was able to justify this decision with the results of shear tests performed on the UHPC girders. This bridge opened to traffic in October 2008 [2].

### 2.2.3 Jakway Park Bridge

Over the past few years the Federal Highway Administration has begun taking steps towards the implementation of ultra-high performance concrete technology on the U.S. highway system. As part of this initiative the FHWA investigated possible applications for the use of UHPC in highway structures. One of the results of FHWA's work is a UHPC decked girder. This pi-girder (Fig. 2-1) was used in the construction of the nation's third UHPC bridge in Buchanan County, Iowa.

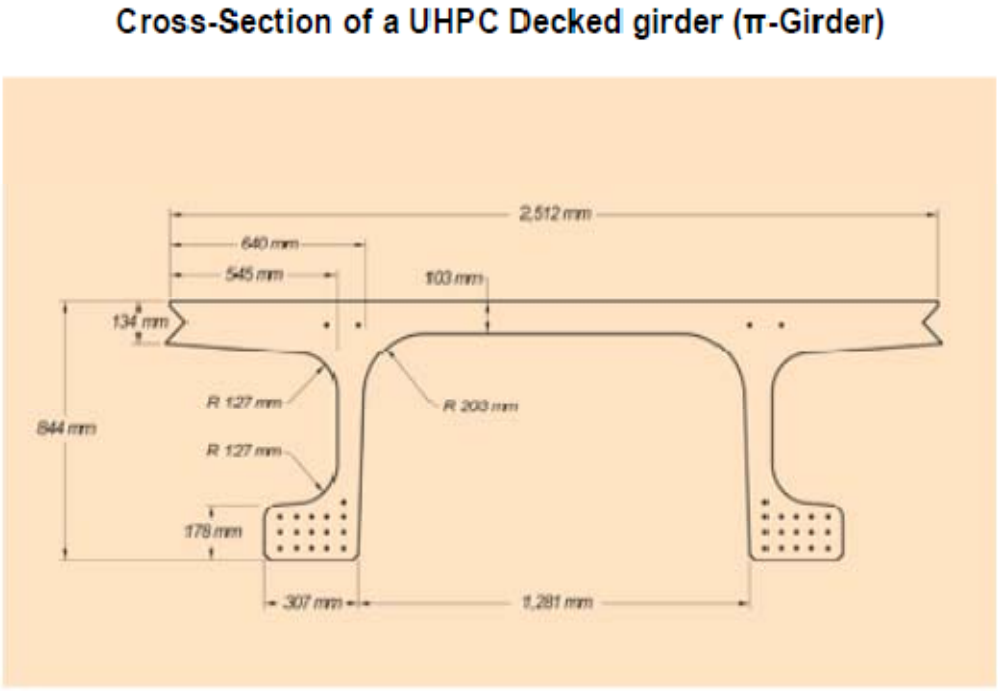


**Figure 2-1. This diagram shows the proposed 2nd generation component designed to span up to 30 meters (98 feet) while allowing for overnight bridge construction or reconstruction [6].**

The Jakway Park Bridge, with a UHPC center span of 51 feet, is a major step away from the previous two UHPC bridges. Instead of modifying an existing girder cross-section, the pi-girder section was developed by the FHWA from the

ground up to take advantage of the superior mechanical and durability properties of ultra high performance concrete. In addition to the structural performance of the pi-girder, design consideration was given to the application of accelerated bridge construction techniques. Tests of the resulting pi-girder section show that the primary shear and flexural properties can be predicted by basic engineering principles. For a span length of up to 87 ft, this section is capable of satisfying the requirements of the *AASHTO LRFD Bridge Design Specifications* [6].

The construction of the Jakway Park Bridge represents several other advances in the application of UHPC to highway structures in the U.S. In the previous two UHPC bridges, the girders were precast in the controlled setting provided by the prestressing plant. The material supplier, Lafarge, recommends that UHPC members are steam-cured following their casting. Even under the most ideal conditions, this is a difficult task to accomplish on the job-site. The designers and constructors of the Jakway Park Bridge worked together to overcome this obstacle and develop a casting and curing regime that satisfied all parties interested. As a result this project was the first to use a ready-mix concrete truck to batch the UHPC on-site. The prestressed girders were cast-in in a manner typical to prestressed construction and cured at ambient temperatures. After the concrete achieved a 5.1 ksi strength (as determined by match-casted cylinders) the forms were removed. The girders continued to cure at ambient temperatures until they achieved 14.5 ksi. At this point the strands were released and a steam treatment regimen began. This stream treatment lasted for about two days at

190$^{o}$F and 95% relative humidity. The final compressive strength of the beams was 21.5 ksi [2,6,7]

### 2.2.4 Canandaigua Outlet Bridge

The final bridge in this discussion makes use of ultra high performance concrete in a different manner. It is a traditional prestressed concrete bridge that was designed to replace an existing steel bridge. UHPC was used to connect the bridges longitudinally. The designers decided to create these joints between the precast deck bulb-tee girders to address concerns they had over regarding durability of the girders. It was not UHPC's high strength, but the short curing time and high early strength gains that dictated their decision to use UHPC. The designers did appreciate the higher strength of the UHPC, but their compressed schedule made them appreciate the high-early strength gains even more. They feel that their decision to use UHPC in this application will provide benefits in the long run. With UHPC in the joints, this high traffic bridge is less likely to need an increased inspection schedule in the future [8].

### 2.2.5 Seoul Footbridge of Peace

The Seonyu footbridge in South Korea consists of a concrete arch component which supports two steel approach spans of 30 m (98.4 ft) each. The bridge spans 120 m (394 ft) and carries pedestrian traffic on the two approach spans and directly on the middle 60 m (197 ft) of the arch. The arch is made from Ductal® and has a pi-shaped cross section. The design of the footbridge included a dynamic analysis of the arch. This analysis revealed natural frequencies of the bridge which would make people uncomfortable while crossing

it. To address this issue tuned mass dampers (TMDs) were deigned to damp the vibrations of the modes next to the natural frequency caused by a pedestrian. The frequencies of the bridge were determined through direct analysis and through measurements made on the bridge. A total of four TMDs were installed on the bridge to keep the vertical and horizontal accelerations within the targeted comfort criteria. In this application, the unique characteristics of UHPC that allowed for a smaller and, therefore, lighter cross-section also introduced vibrations issues that are usually only seen in similar steel structures [9].

## 2.3 UHPC and Design

Several American universities have begun performing research on UHPC. Much of this research involves the material characterization and modeling of the new material. Other research involves full-scale testing of UHPC structures to model flexural behavior in a girder or the blast impacts on a slab. These areas of focus seem to be more plentiful when compared to research into the theory regarding the design of UHPC structures. Some literature has come out of MIT concerning the modeling of UHPC structures, but this seems to be the extent of it [10].

The bulk of the research into UHPC for material properties, full scale testing and design theory has been performed by the FHWA. In particular, the FHWA has produced numerous papers detailing the mechanical characterization and structural behavior. From the results of these papers the FHWA has been able to shed some light into the design theory of UHPC structures. With respect to prestressed concrete structures, the designer needs to consider the fairly linear stress-strain curve of UHPC and how this impacts the internal stress-distribution

of the beam. The Whitney-stress block no longer accurately describes the idealized stress block of the UHPC beam. The FHWA proposes that depth of the stress block be taken equal to the full depth of the neutral axis (Fig. 2-2). With this assumption and the appropriate adjustments, the FHWA claims that slabs and beams made of UHPC can be design to satisfy the *AASHTO LRFD Bridge Design Specifications.* However, the bridge designer must note that the current AASHTO specification limits the compressive strength of concrete to 70 MPa (10 ksi) for most applications. It does allow the use of higher values for the compressive strength of concrete under special circumstances and usually only after extensive testing [11,12].

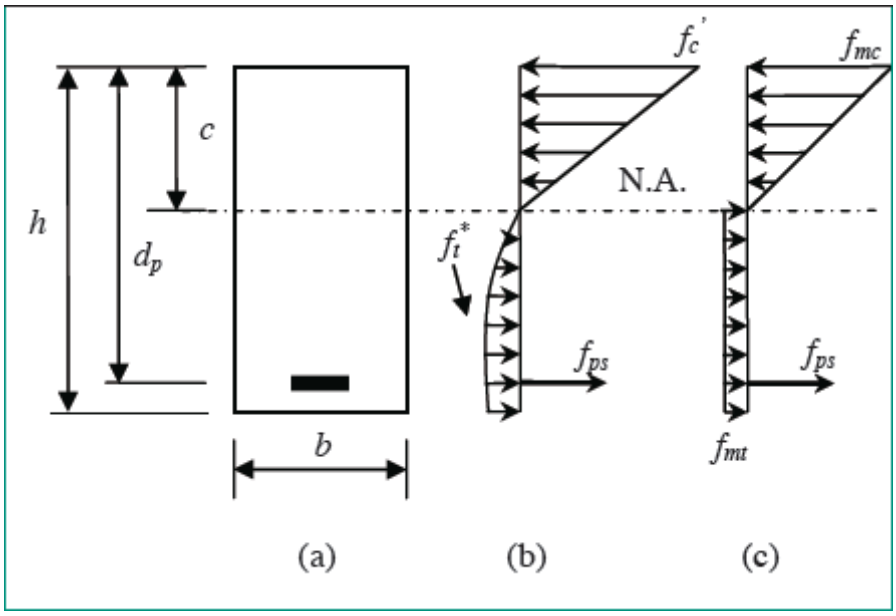


**Figure 2-2. Idealized internal stress distribution for a prestressed beam [11].**

## 2.4 Conclusion

The superior properties of UHPC lend itself to many applications. In the world of bridge builders this new material means greater spans, shallower section depths, reduced self-weight and a reduced need for steel reinforcing. The ability to span greater distances means fewer joints and bearings and, therefore, reduced maintenance over the lifetime of the structure. The characteristics of UHPC are allowing engineers and designers to create new classes of structural elements. The examples reviewed in this paper are just a sample of what is possible as we enter a new age of design with smart materials. However, before any of these structures can be implemented on a regular basis much more development of the UHPC flexural methodology needs to be conducted. Until UHPC is directly addressed in the applicable codes and specifications, it will remain the source of interesting one-off structures and not realize its full-potential.

## References

[1] B.A. Graybeal, Material property characterization of ultra-high performance concrete., (2007).

[2] B.A. Graybeal, UHPC making strides, Public Roads. 72 (2009).

[3] T.M. Ahlborn, What you should know about UHPC, National Precast Concrete Association. (2008).

[4] W.A. Endicott, A Whole New Cast, Aspire. (2007).

[5] D. Bierwagen, Ultra-high performance concrete in Iowa, HPC Bridge Views. (2009) 1-3.

[6] B.A. Graybeal, TECHBRIEF - Structural behavior of a 2nd generation UHPC pi-girder, FHWA, 2009.

[7] B. Keierleber, FHWA, Iowa Optimize Pi Girder, Aspire. (2010).

[8] C.A. Shutt, UHPC joint provides new solution, Aspire. Fall (2009).

[9] M. Behloul, K.C. Lee, Ductal® Seonyu footbridge, Structural Concrete. 4 (2003) 195-201.

[10] M. Soh, Model-based design of a ultra high performance concrete prototype highway bridge girder, Massachusetts Institute of Technology, 2003.

[11] H. Garcia, B.A. Graybeal, TECHBRIEF - Analysis of an ultra-high performance concrete two-way ribbed bridge, FHWA, 2007

[12] B.A. Graybeal, Flexural Behavior of an Ultrahigh-Performance Concrete I-Girder, Journal of Bridge Engineering. 13 (2008) 602-610.

# Chapter 3 – Residual Compressive Strength of Ultra-High Performance Fiber-Reinforced Concrete with Polypropylene Fibers after Exposure to Elevated Temperatures


## Abstract

This chapter presents the results of a study on the effect of elevated temperatures on the compressive strength of ultra-high-performance fiber-reinforced concrete (UHPFRC). Two different mixtures of a commercially available UHPFRC were considered in this study. The standard mixture offered by the manufacturer incorporates only steel-fibers to improve the tensile properties of the concrete. The enhanced mixture, which is of primary focus in the study, incorporates additional polypropylene fibers to improve the fire-resistance behavior. Specimens from each mixture were cast into 76 mm (3 in.) diameter cylinders and 51 mm (2 in.) cubes. After exposure to elevated temperatures ranging from 200 to 600$^{o}$C (392 to 1112$^{o}$F) and for durations ranging from 5 minutes to 6 hours, the residual compressive strength was measured. The fire-resistant mixture exhibited no explosive spalling during heating but demonstrated reduced compressive strength at temperatures over 200$^{o}$C (392$^{o}$F). Durations greater than one hour had little effect on the residual compressive strength of the cylinders. Unlike the cylinders, the residual strength of the cubes was affected by the heating duration. The standard mixture exhibited explosive spalling at oven temperatures above 250$^{o}$C (482$^{o}$F) which

demonstrates that incorporation of polypropylene fibers prevents the occurrence of explosive spalling in UHPFRC at temperatures up to 600$^{o}$C.

## 3.1 Introduction

In recent years, developments in concrete technology have lead to a new class of concrete known as ultra-high performance concrete (UHPC). UHPC is a class of concretes that exhibit very high compressive strengths, exceptional durability and other desirable characteristics. These properties are achieved using high-quality ingredients and optimized mix designs. The batching, mixing, placing and curing of these mixes often require special attention above that of normal strength concrete [1]. While there are several recently developed concretes that could be classified as UHPC, a universally accepted definition of UHPC has yet to be adopted. However, UHPC is generally considered to be a material with a cement matrix containing steel fibers which produces compressive strength exceeding 150 MPa (22 ksi) with significant ductile behavior [2,3,4].

In order to achieve such high compressive strengths, the particle packing density of the material has been optimized to reduce the porosity. It is well established that there exists an inverse relationship between the porosity and compressive strength of concrete [5,6,7]. In order to achieve an optimized particle packing effect, researchers have developed concrete mixes that are primarily powdered fines with water, chemical and mineral admixtures, and which do not contain any coarse aggregate. Additionally, a UHPC typically has a water-cementitious material ratio (*w/cm*) below 0.2. The reduced porosity of UHPC also improves its durability in aggressive environments and self-sealing of microcracks [8].

However, this reduced porosity increases the occurrence of explosive spalling when it is exposed to elevated temperatures. Normal strength concrete, when exposed to elevated temperatures performs fairly well. It is a non-combustible material that does not give off any fumes when heated, retains a large portion of its compressive strength and serves to dissipate heat in a fire. Its porous structure provides an environment that allows any built up pore pressure/internal pressure to escape. The virtual elimination of the pore spaces from the cement matrix in UHPC effectively disables the release of the internal pressure and will cause the concrete to explosively spall. This process is described as moisture clogging and can be seen in Fig.3-1. This is a very undesirable side effect and one that puts limitations on the use of UHPC as a structural material. However, when the polypropylene fibers are added to UHPC, they allow for the creation of a pore structure when the fibers begin to melt at $180^{o}$C. This will vent the pressure before explosive spalling can occur.

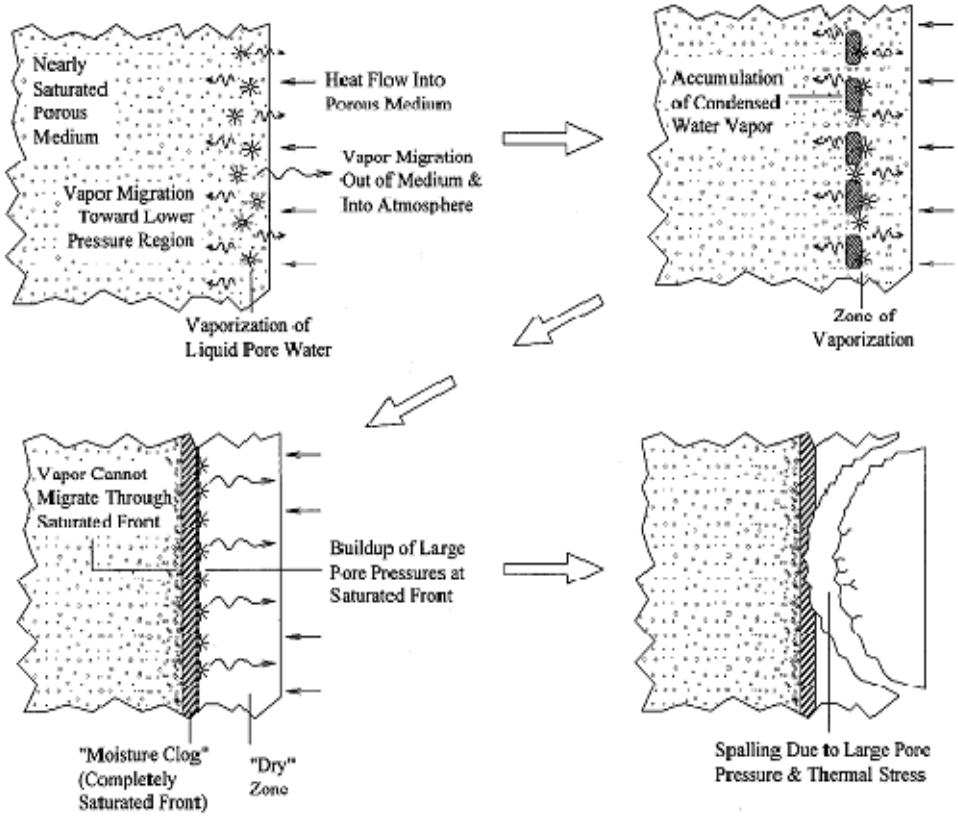


**Figure 3-1. Moisture clog spalling [9].**

The UHPC studied in the research program is a commercially available product named Ductal® that was developed by the three French companies Lafarge, Bouygues and Rhodia.

## 3.2 Experimental Methodology

In this study, the following factors were considered as having potential effects on the residual compressive strength of UHPC:

- Water-cementitious materials ratio (*w/cm*) (0.18 and 0.19);
- Exposure duration (0, 1, 2, 3, 4 and 6 hours);
- Exposure temperature (200, 300, 400, 500 and 600$^{o}$C).

### 3.2.1 Materials and Mixture Proportioning

The mixture consists of a premix, high-range water-reducing admixture (HRWA), water, steel fibers and polypropylene fibers. Table 3-1 shows the mix constituents and their amounts. The premix was provided by the manufacturer and it consists of Portland cement, silica fume (SF), ground quartz and fine sand. Silica fume is the smallest particle in the premix. It is small enough to fill the interstitial voids between the cement and the ground quartz particles. Ground quartz has an average particle size of 10 micrometers. Portland cement is the next largest particle with a diameter of 15 micrometers. Fine sand is the largest particle in the premix. Generally, it is between 150 and 600 micrometers. The particle size distribution of the premix is designed by the manufacturer to achieve an increased particle density without sacrificing workability.

Both mixtures considered in this study have a high density of fibers at 2% by volume. Two types of fibers were used to produce the UHPC mixtures. One is a high-carbon steel fiber (Figure 3-2) and the other is a polypropylene (PP) or poly-vinyl alcohol (PVA) fiber (Figure 3-3). The steel fibers are 13-15 mm long and have a diameter of about 0.2 mm. The steel fibers are crimped along their length to improve their bond to the cement paste. The size, deformed shape and amount of fibers are the result of extensive testing over the last few decades [10].

**Table 3-1. Mix constituents. Ductal-FM® is the standard UHPC offered by Lafarge. Ductal-AF® is the polypropylene fiber containing mixture offered by Lafarge.**

| | Ductal-FM® | | Ductal-AF® | |
|---|---|---|---|---|
| **Material** | **Amount kg/m$^3$ (lbs/yd$^3$)** | **% by weight** | **Amount kg/m$^3$ (lbs/yd$^3$)** | **% by weight** |
| **Premix** | 2198 (3705) | 86.4 | 2198 (3705) | 86.5 |
| **Superplasticizer** | 30.0 (50.6) | 1.18 | 30.0 (50.6) | 1.18 |
| **Accelerator** | 30.0 (50.6) | 1.18 | 30.0 (50.6) | 1.18 |
| **Steel Fibers** | 156 (263) | 6.13 | 151 (253) | 5.91 |
| **Polypropylene fibers** | -- | -- | 5.02 (8.46) | 0.20 |
| **Water** | 129 (217) | 5.07 | 129 (217) | 5.08 |


**Figure 3-2. Steel fibers.**


**Figure 3-3. Polypropylene fibers.**

### 3.2.2 Specimen Preparation

A total of five 0.0165 $m^3$ (0.583 $ft^3$) batches each were made for this study: four batches containing steel and polypropylene fibers, and one batch without steel fibers. The proportions of the four batches containing polypropylene fibers were identical with the exception of one with a higher *w/cm*. The premix used in all batches came from the same shipment and was about 7 months old at the time of batching. All batches were produced over a two week period and were prepared in the same manner. The mixing procedure is based on guidance provided by the manufacturer; however some of the mixing durations were adjusted based on the environmental conditions in the concrete laboratory. The following is the general mixing procedure followed in this study:

1. Weigh all constituent materials.
2. Place premix in mixer pan and mix for 2 minutes.
3. Add water (with half of the HRWA) to premix slowly over 2 to 4 minutes.
4. Mix 1 minute.
5. Add remaining HRWA to premix over 30 seconds.
6. Mix 1 minute.
7. Add accelerator over 1 minute.
8. Mix for 1 minute or until UHPC becomes a thick paste. Time will vary.
9. Add fibers to the mix slowly over 2 minutes.
10. Mix for 1 minute or until the fibers are well dispersed.
11. Remove from mixer.

The total mix time never exceeded 35 minutes. Adjustments to the mixing durations of each batch could vary by as much as 10 minutes which is hypothesized to be a result of the humidity and temperature variations in the laboratory. The laboratory is an unconditioned space and the ambient conditions fluctuate due to the presence of various pieces of equipment (e.g. freeze-thaw table). Temperature and relative humidity conditions found in the laboratory ranged from 20 to 27$^{o}$C (68 to 80$^{o}$F) and 55 to 72%RH.

Once the fresh UHPC was removed from the mixer, a flow test was performed to determine the rheological properties of each batch. This test followed the general

procedures outlined in ASTM C1437. In each batch the flow exceeded the capacity of the flow table.

All specimens were cast in the same manner using a vibratory table. The table vibrated at 60 Hz and had an adjustable amplitude. Due to the relatively high flowability of the batches, the duration of the fresh specimens on the vibratory table were kept to a minimum to avoid over-consolidation and separation of the steel fibers from the fresh concrete. Each mold was filled in 3 to 4 lifts. The cylinders were cast in 2-in plastic molds and the cubes were cast in 2-in. brass molds. Each batch created 48 cylinders and 48 cubes. Not all of the cubes were used for compression testing. The casting of all specimens was completed approximately 30 to 45 minutes after the batch was removed from the mixer.

After casting, the specimens were covered in a heavy plastic sheet and left to set for 40 to 48 hours before they were demolded. The demolded specimens were placed in a steam cure box for curing. The curing always started at room temperature and ambient relative humidity (RH), and was set to reach 90$^{o}$C (194$^{o}$F) and 95%RH, respectively. The target values were typically reached after approximately 90 minutes. The total curing time was 48 hours after which the UHPC specimens were removed from the steam cure box and left to cool to laboratory conditions.

To prepare the cylinders for compression testing, the non-cast end of the cylinders was cut off using a masonry wet saw. This served to provide a flat top surface that was parallel to the cast end and perpendicular to the specimen sides. The planeness for each specimen was measured using the apparatus

shown in Fig. 3-4. Four diametrically opposed pairs of points were marked on the cut surface (Fig. 3-5). The relative difference in height of each of the pairs was measured using the dial gauge setup. This number was divided by the distance between the pair to find the angle of out-of-planeness for the specimen. If the average of the four angles was greater than $1^{o}$, the specimen was re-cut and measured. A summary of these measurements for all specimens is shown in Fig. 3-6 Once the specimens passed the planeness check, they were considered ready for the heat treatment. Four to eight specimens were set aside from each batch to serve as the controls. These specimens did not undergo any heating and were maintained at laboratory conditions until testing. In order to facilitate the statistical analysis of the specimens, the controls are labeled as $25^{o}$C ($77^{o}$F) and 0 hours duration.


**Figure 3-4. Planeness measuring apparatus.**

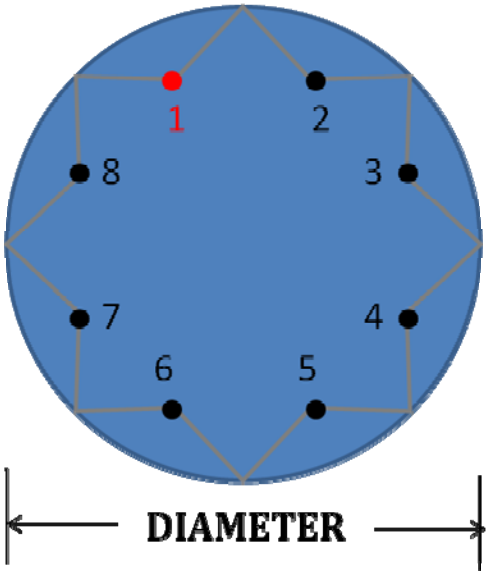


**Figure 3-5. Layout of points used to determine the end planeness of cylinder.**

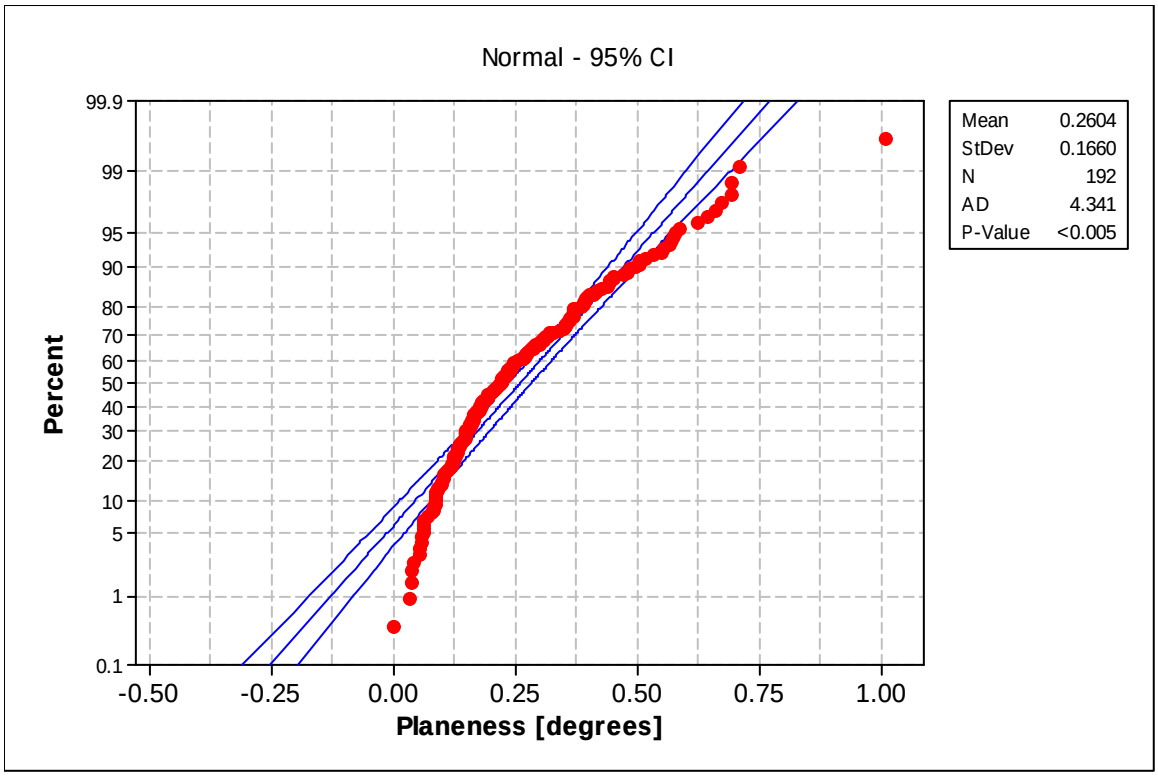


**Figure 3-6. Probability plot of planeness measurement for all specimens.**

### 3.2.3 Heating of Specimens

An ignition oven was used to heat all the specimens in this study. This oven draws ambient air through four ceramic tube supports located on the chamber floor. This heated and oxygenated air then interacts with the test specimens. Figure 3-8 shows the heating history of the ignition oven. The specimens were heated from room temperature to the target temperature at the maximum furnace heating rate of 5$^{o}$C/min (9$^{o}$F/min). The target temperature was maintained until the target duration was achieved. The specimens were then removed from the oven and allowed to cool at room temperature. For the heated specimens, a duration of 0 hours indicates that the specimens were removed once the target temperature was reached. A summary of the specimen heating matrix is shown in Table 3-2.

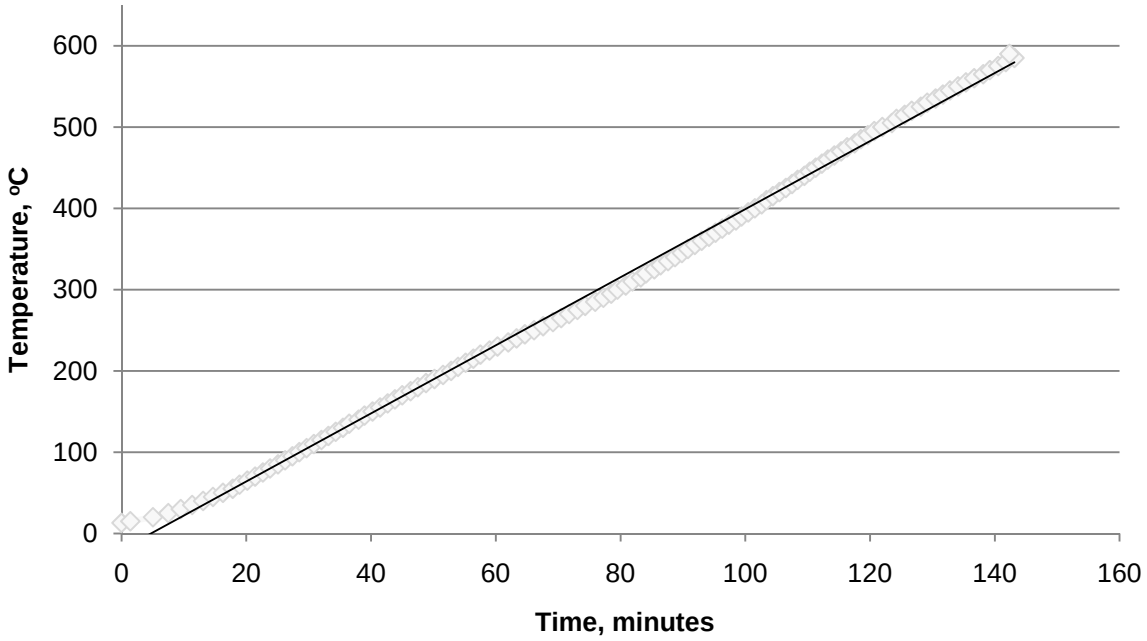


**Figure 3-8. Ignition oven heating rate. This curve represents the summary of several trials and was used to determine the heating rate of the oven.**

**Table 3-2. Specimen heating matrix. Batch 130 had *w/cm* = 0.193. For batches 132, 137 & 139 *w/cm* = 0.180. Note that the batch number refers to the Julian date on which the batch was cast.**

| | | Duration, hours | | | | | |
|---|---|---|---|---|---|---|---|
| Temperature, °C (°F) | | 0 | 1 | 2 | 3 | 4 | 6 |
| | 200 (392) | 132 | 132, 137, 139 | 130 | 132, 137 | 130 | 130 |
| | 300 (572) | 132 | 137, 139 | - | 137 | - | - |
| | 400 (752) | - | 137 | 130, 132, 137, 139 | 137 | 130 | 130, 132, 139 |
| | 500 (932) | - | 137 | 132 | 137 | - | 132 |
| | 600 (1112) | - | 137, 139 | 130, 132 | 137 | 130 | 130, 132 |

### 3.2.4 Determination of strength of concrete

A Tinius-Olsen load frame rated at 1330 kN (300 kips) was used for the testing of all the specimens. The capacity of the load frame was greater than 150% of the expected load in the compressive strength testing, therefore the stiffness of the load frame was considered adequate. The load frame was calibrated 4 months prior to testing effort. A post-testing calibration report indicates that the load frame maintained its calibration throughout the testing regimen. The load platen used was 254 mm (10-in.) diameter which was assumed as adequate to transfer the load into the test specimen [11].

The compression testing generally followed the procedure outlined in ASTM C39. However, due to the expected high compressive strengths of the specimens, a load rate of 1MPa/sec (150 psi/sec) was used. This equates to about 4 times the suggested load rate in the ASTM standard. The effect of this increased load rate for UHPC has been studied and found to provide no influence on the measured compressive strength and allows for reduced testing time [12].

## 3.3 Results and Discussion

### 3.3.1 Residual Compressive Strength

The results of the compressive strength tests of the control specimens for each batch is shown in Table 3-3. The residual compressive strength, $f_{RES}$ of each specimen is defined by the relationship:

$$f_{RES} = f_{TEMP}/f_{25}$$

Where $f_{TEMP}$ is the compressive strength of the heated specimen (i.e. $f_{200}$, $f_{300}$, $f_{400}$, $f_{500}$ and $f_{600}$) and $f_{25}$ is the average compressive strength of the control specimens. The heated specimens of each batch are only compared to the controls of their batch. The residual compressive strength of the heated specimens is shown in Figs. 3-9 and 3-10.

**Table 3-3. Compressive strength results of controls. Ductal-FM® refers to the standard mix design and Ductal-AF® is the enhanced mixture that contains polypropylene fibers.**

| Mix | w/cm | Shape | Number of Specimens | Mean Compressive Strength, MPa | Standard Deviation, MPa | COV |
|---|---|---|---|---|---|---|
| **Ductal-FM®** | 0.180 | Cylinder | 28 | 151.6 | 13.22 | 8.72% |
| **Ductal-AF®** | 0.180 | Cylinder | 17 | 147.7 | 13.29 | 9.00% |
| | | Cube | 8 | 180 | 12.94 | 7.19% |
| | 0.193 | Cylinder | 4 | 136.9 | 16.07 | 11.74% |
| | | Cube | 9 | 140 | 10.67 | 7.61% |

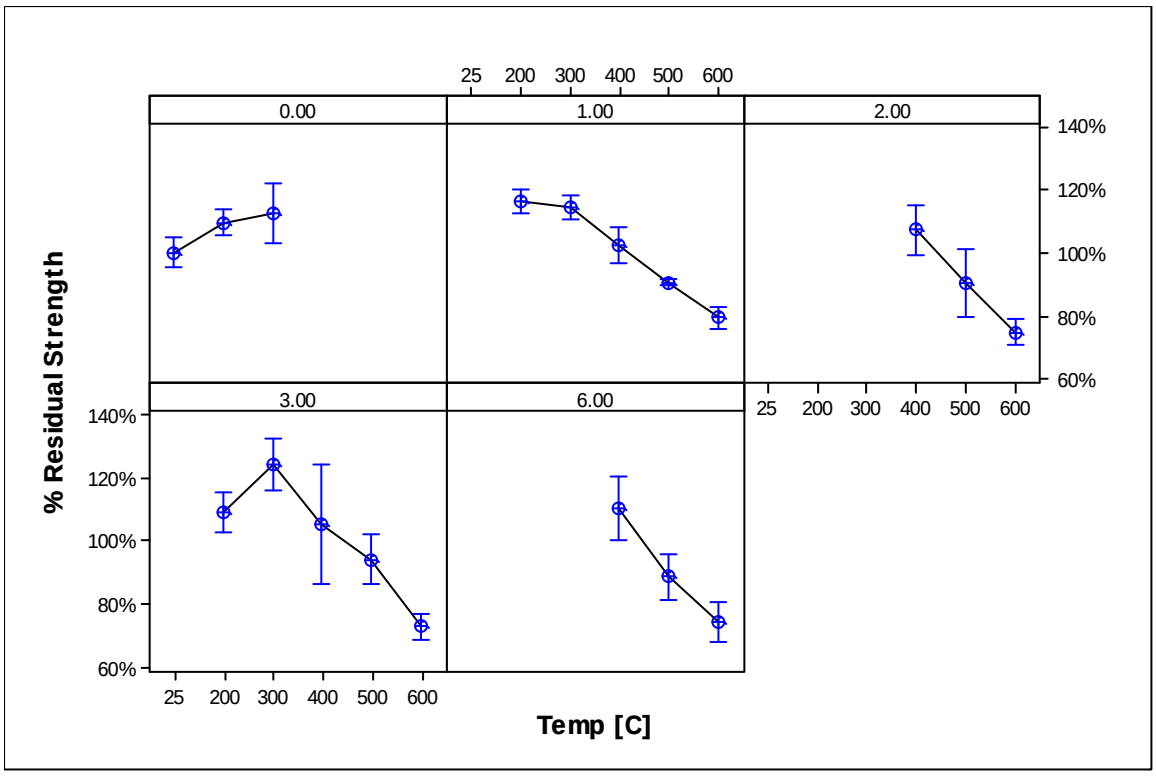


**Figure 3-9. Residual strength of cylinders. Interval plot of % residual strength. Each panel represents a different heating duration measured in hours.**

### 3.3.2 Statistical Analysis

Analysis of variance (ANOVA) was performed using a general linear model (GLM). Heating duration, temperature and *w/cm* ratio were selected as factors, whereas the residual compressive strength was a dependent variable.

The validity of the GLM depends on the following assumptions made about the errors:

- The errors are normally distributed with a mean of zero.
- The error variance does not change for different levels of a factor or according to the values of the predicted response.
- Each error is independent of all other errors.

These assumptions were checked and were satisfied for each trial.

#### 3.3.2.1 Cylinders

A comparison of the three batches with a *w/cm* = 0.180 was used to determine if the three batches (132, 137 and 139) can be treated as equals. The average compressive strengths for the control specimens from these three batches were compared using a two-sample t-test with $\alpha$-level of 0.05. The results are summarized in Table 3-4. The null hypothesis, $H_0$, is that the average strengths, $\mu_X$ and $\mu_Y$, of the batches are equal, i.e. the difference is equal to zero:

$$H_0: \mu_X - \mu_Y = 0$$

One can notice in Table 3-4, that 95% confidence interval for difference of each of the pairings contains zero value, and the p-value for the difference is greater than the $\alpha$-level. Therefore one cannot reject the null hypothesis that batches are different which justifies treating these three batches as one group with *w/cm* equal to 0.180.

**Table 3-4. Results of t-test for batches 132, 137 and 139.**

| Batch Pairing | 95% Confidence Interval for difference | t-value | p-value | $H_o$ |
|---|---|---|---|---|
| **132 & 137** | (-13.55, 17.04) | 0.28 | 0.790 | Cannot reject |
| **132 & 139** | (-13.68, 19.83) | 0.41 | 0.691 | Cannot reject |
| **137 & 139** | (-16.29, 18.96) | 0.17 | 0.868 | Cannot reject |

The following hypotheses were tested using a 0.05 level of significance (p-value):

> $H_o$': there is no difference in the mean residual compressive strength of the specimens when heated at different temperatures;

***$H_o$''***: there is no difference in the mean residual compressive strength of the specimens when heated at the same target temperature for different durations;

***$H_o$'''***: there is no difference in the mean residual compressive strength when different *w/cm* ratios are used.

The results of the ANOVA are summarized in Tables 3-5 and 3-6.

Prior to running the GLM, the test specimens were balanced by forming the following groupings to test the various three hypotheses:

I. Specimens which were heated for 1 or 3 hours at 200, 300, 400, 500 or 600$^{o}$C
II. Specimens which were heated for 1, 2, 3 or 6 hours at 400, 500 or 600$^{o}$C
III. Specimens which were heated for 0, 1 or 3 hours at 200 or 300$^{o}$C
IV. Specimens from the two *w/cm* ratios which were heated for 2 or 6 hours at 400 or 600$^{o}$C

**Table 3-5. Summary of ANOVA for cylinders for Groups I, II and III.**

| Group | Variable | Degrees of Freedom | Adjusted Mean Square | Computed F | p-value | Significant |
|---|---|---|---|---|---|---|
| I | **Duration** | 1 | 0.00053 | 0.15 | 0.697 | No |
| | **Temp** | 4 | 0.32721 | 94.32 | 0.000 | Yes |
| | **Interaction** | 4 | 0.01659 | 4.78 | 0.002 | Yes |
| | **Error** | 50 | 0.00347 | - | - | - |
| II | **Duration** | 3 | 0.00224 | 0.31 | 0.821 | No |
| | **Temp** | 2 | 0.56974 | 77.82 | 0.000 | Yes |
| | **Interaction** | 6 | 0.00519 | 0.71 | 0.643 | No |
| | **Error** | 66 | 0.00732 | - | - | |
| III | **Duration** | 2 | 0.009231 | 2.68 | 0.082 | No |
| | **Temp** | 1 | 0.025671 | 7.45 | 0.010 | Yes |
| | **Interaction** | 2 | 0.025580 | 7.43 | 0.002 | Yes |
| | **Error** | 36 | 0.003444 | - | - | - |

**Table 3-6. Summary of ANOVA for cylinders in Group IV.**

| Group | Variable | Degrees of Freedom | Adjusted Mean Square | Computed F | p-value | Significant |
|---|---|---|---|---|---|---|
| IV | **Duration** | 1 | 0.00008 | 0.01 | 0.922 | NO |
| | **Temp** | 1 | 0.80899 | 94.57 | 0.000 | YES |
| | **w/cm** | 1 | 0.07034 | 8.22 | 0.007 | YES |
| | **Duration* Temp** | 1 | 0.00285 | 0.33 | 0.568 | NO |
| | **Duration * *w/cm*** | 1 | 0.00104 | 0.12 | 0.730 | NO |
| | **Temp **w/cm*** | 1 | 0.01634 | 1.91 | 0.176 | NO |
| | **Duration* Temp * *w/cm*** | 1 | 0.00002 | 0.00 | 0.962 | NO |
| | **Error** | 35 | 0.00855 | - | - | - |

A simplified summary of the main effects of the heating temperature and duration on the residual compressive strength are shown in Fig. 3-10. This figure shows that the effect of heating beyond 1 hour has no significant impact on $\mathbf{f_{RES}}$ of the cylinders. It also shows that the general trend of the effect of temperature on $\mathbf{f_{RES}}$ for UHPC with PP-fibers is similar to that of other concretes as shown in Fig. 3-11.

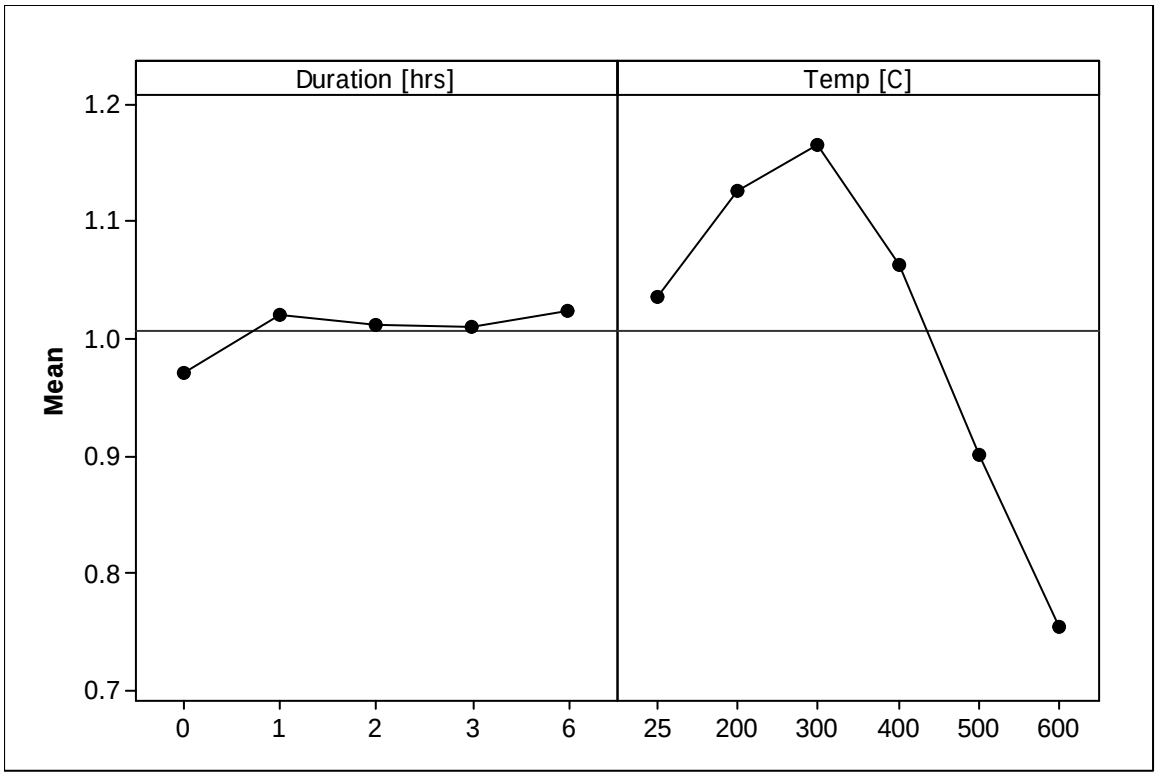


**Figure 3-10. Main effects plot for percent residual strength.**

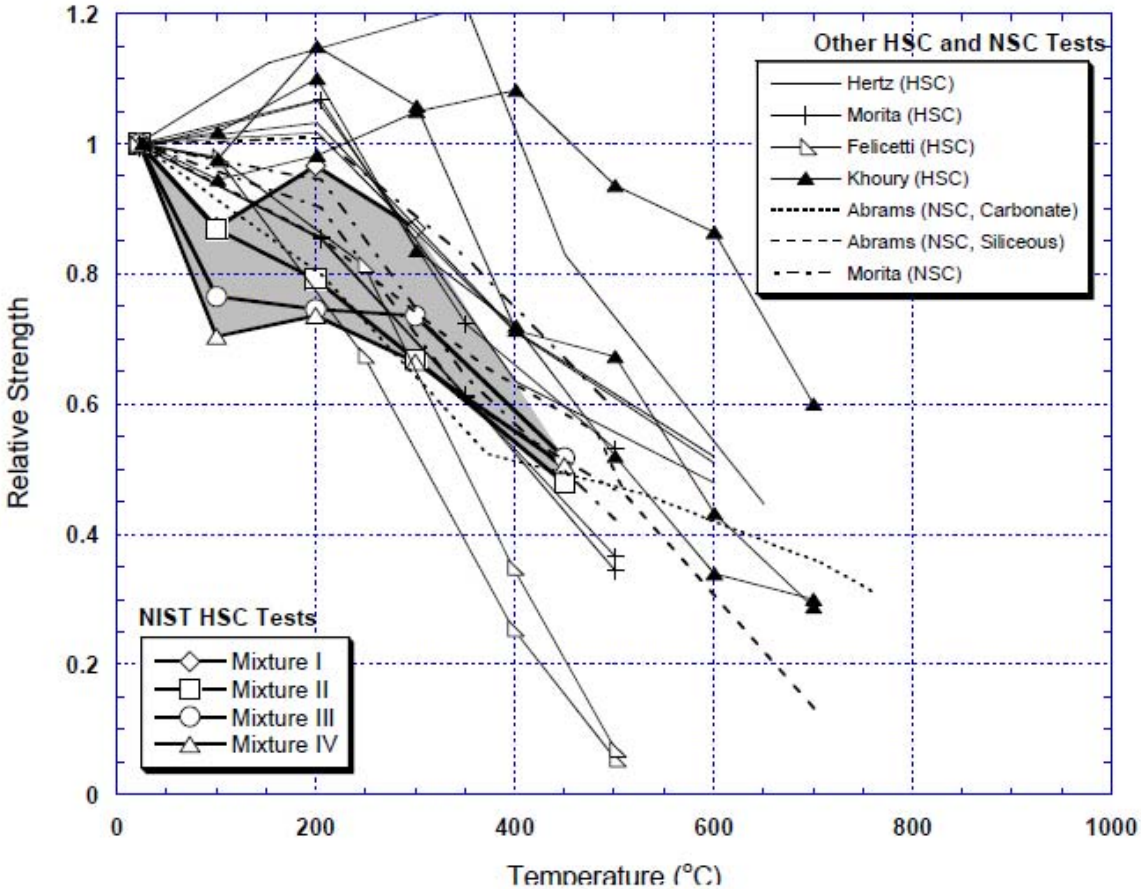


**Figure 3-11. $f_{RES}$ for other types of concrete. [13]**

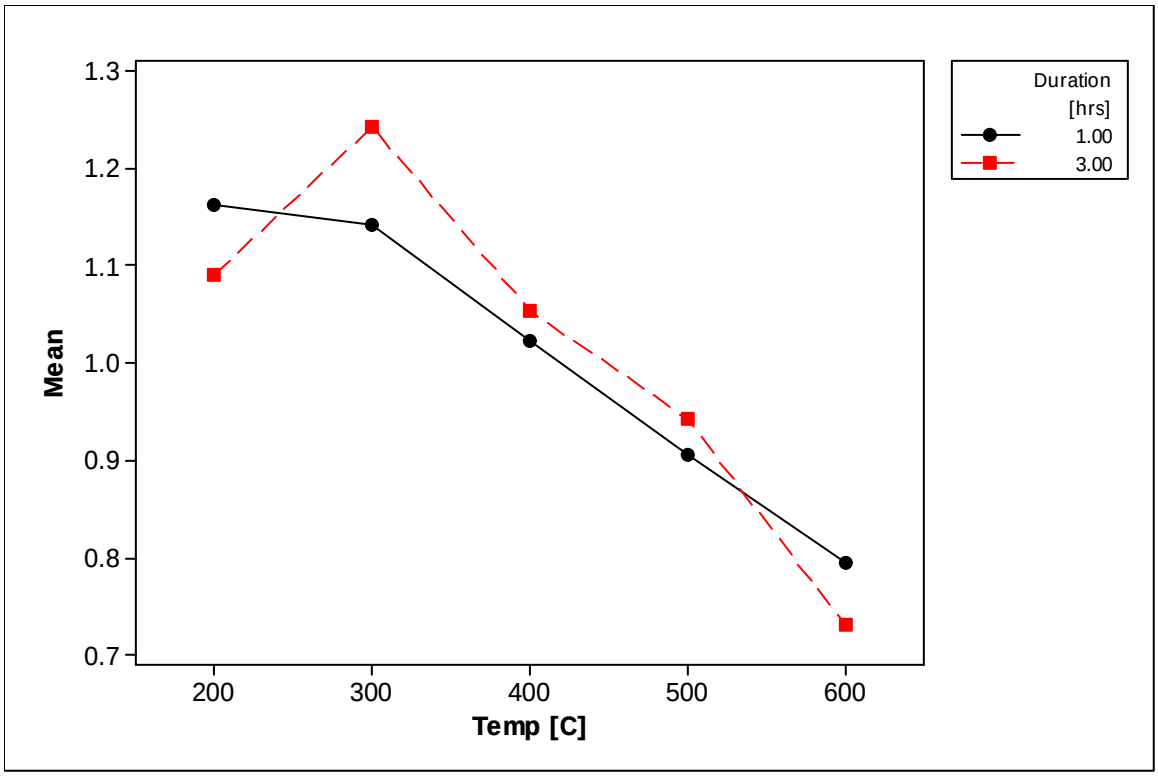


**Figure 3-12. Interaction plot for Group I.**

The interaction plot of duration and temperature for Group I (Fig. 3-12) shows that when heating for 1 hour the residual strength declines for all temperatures. However, when heating for 3 hours the residual strength first increases from 200 to 300$^{o}$C [392 to 572$^{o}$F] and then decreases in a similar manner observed in the 1 hour heating.

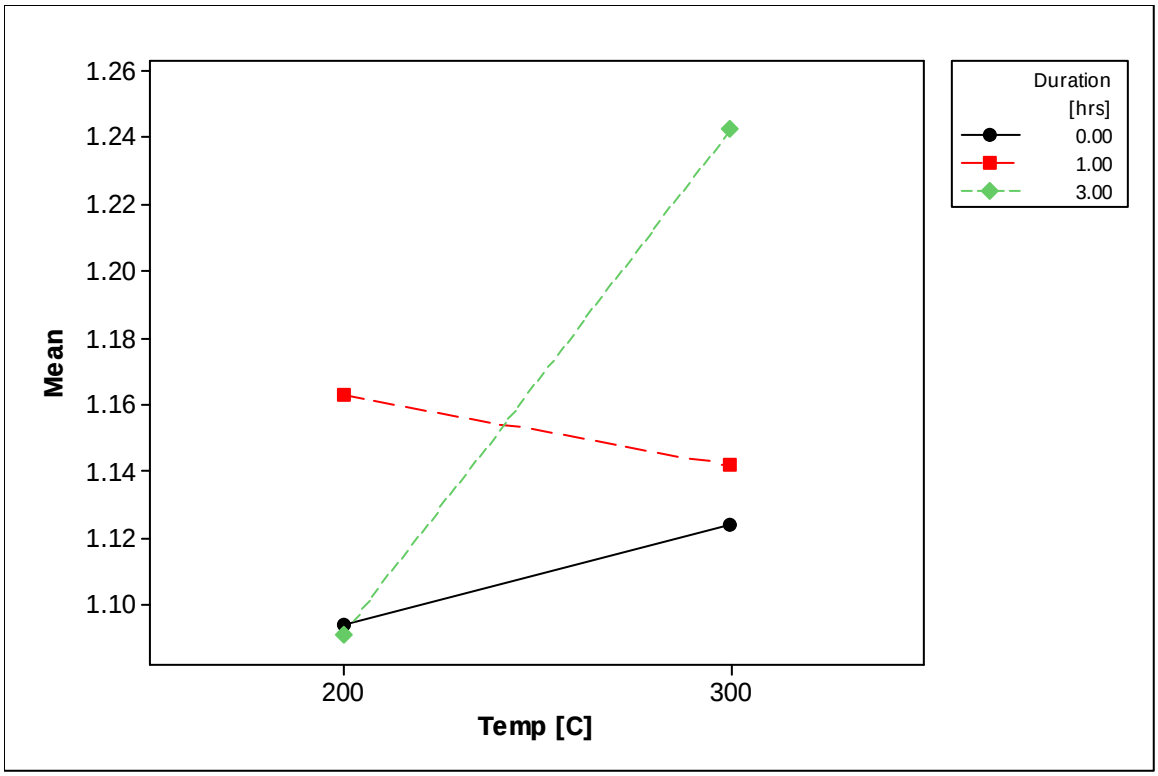


**Figure 3-13. Interaction plot for Group III.**

The interaction plot of duration and temperature for Group III (Fig. 3-13) contributes more information on the effect of the duration for the 200 and 300$^{o}$C [392 to 572$^{o}$F] samples from Group I. It includes a third heating duration of zero hours which are samples that were removed from the oven at the instant that target temperature was reached.

From these results one can see that for all three groupings the duration was not significant. The lack of any significant effect on residual strength by the varying duration suggests that the specimens were heated through their entirety after one hour. Additionally, the duration of exposure at elevated temperatures practically guarantees that the test samples are heated uniformly and a uniform

temperature is reached within the whole specimen volume. As expected, the temperature was a significant factor.

### 3.3.2.2 Cubes

A subset of 51 mm (2-in.) cubes from batches 130 and 132 underwent compression testing. These specimens were also used to test the various hypotheses presented earlier. Prior to running the GLM, the test specimens were balanced by forming the following groupings:

V. Specimens from the two w/cm ratios which were heated for 2 or 6 hours at 400 or 600$^{o}$C.

VI. Specimens from Batch 130 (w/cm = 0.193) which were heated for 2, 4 or 6 hours at 200, 400 or 600$^{o}$C.

The results of the ANOVA for these groups is shown in Table 3-7.

**Table 3-7. Summary of ANOVA for test specimens in Groups V and VI.**

| Group | Variable | Degrees of Freedom | Adjusted Mean Square | Computed F | p-value | Significant |
|---|---|---|---|---|---|---|
| V | **Duration** | 1 | 0.03270 | 4047 | 0.044 | YES |
| | **Temp** | 1 | 0.36893 | 50.39 | 0.000 | YES |
| | ***w/cm*** | 1 | 0.39673 | 54.18 | 0.000 | YES |
| | **Duration *Temp** | 1 | 0.02904 | 3.97 | 0.057 | NO |
| | **Duration **w/cm*** | 1 | 0.00073 | 0.10 | 0.755 | NO |
| | **Temp*w/cm** | 1 | 0.02575 | 3.52 | 0.072 | NO |
| | **Duration *Temp*w/cm** | 1 | 0.12904 | 17.62 | 0.000 | YES |
| | **Error** | 26 | 0.00732 | - | - | - |
| VI | **Duration** | 2 | 0.17864 | 16.24 | 0.000 | YES |
| | **Temp** | 2 | 0.71302 | 64.81 | 0.000 | YES |
| | **Interaction** | 4 | 0.22045 | 20.04 | 0.000 | YES |
| | **Error** | 30 | 0.01100 | - | - | - |

The ANOVA shows that the heating duration, temperature and the *w/cm* for the specimens are all significant factors on the residual strength of the test specimen. This differs slightly from the results seen in the cylinders. The heating duration was not a significant factor for the cylinders. This can be attributed to the inherent differences of the two shapes. The cylinders have a shape which readily lends itself to uniform heating along its radius, whereas the cube does not. The non-uniform heating that occurs through the cube results in varying degrees of heating damage in the test specimens.

#### 3.3.2.3 Cylinder-Cube Correlation Factor

In an attempt to further explore the effect of specimen geometry on the residual compressive strength, the residual strength of the cylinders was compared to the residual strength of the cubes from the same heating group. The $\mathbf{f_{res}}$ value of each cylinder was divided by the $\mathbf{f_{res}}$ of each cube from the same group. This iterative process was performed using MATLAB and resulted in the correlation factor, $\mathbf{C_f}$, described by the formula below.

$$\mathbf{C_f = f_{CYL}/f_{CUBE}}$$

The results were then analyzed using statistical analysis similar to that previously mentioned in this paper. In the case of the t-test to compare the $\mathbf{C_f}$ of the two different batches, the p-value is less than the alpha-level, therefore the null hypothesis cannot be rejected and the *w/cm* ratio has no significance on the shape and heating (Table 3-8). The results of the ANOVA (Table 3-9) confirm that the duration and temperature are both significant factors for the correlation

factor as expected. Figure 3-13 shows an interval plot of the correlation factor for the specimens grouped by heating duration and *w/cm* ratio.

**Table 3-8. Results of t-test for cubes and cylinders with *w/cm* = 0.179 and 0.193.**

| 95% Confidence Interval for difference | t-value | p-value | $H_o$ |
|---|---|---|---|
| (-0.0065, 0.0790) | 1.68 | 0.095 | Cannot reject |

**Table 3-9. Summary of ANOVA for test specimens for correlation factor.**

| Variable | Degrees of Freedom | Adjusted Mean Square | Computed F | p-value | Significant |
|---|---|---|---|---|---|
| **Duration** | 2 | 0.30156 | 25.95 | 0.000 | Yes |
| **Temp** | 2 | 0.27504 | 23.66 | 0.000 | Yes |
| **Interaction** | 4 | 0.35952 | 30.93 | 0.000 | Yes |
| **Error** | 181 | 0.01162 | - | - | - |

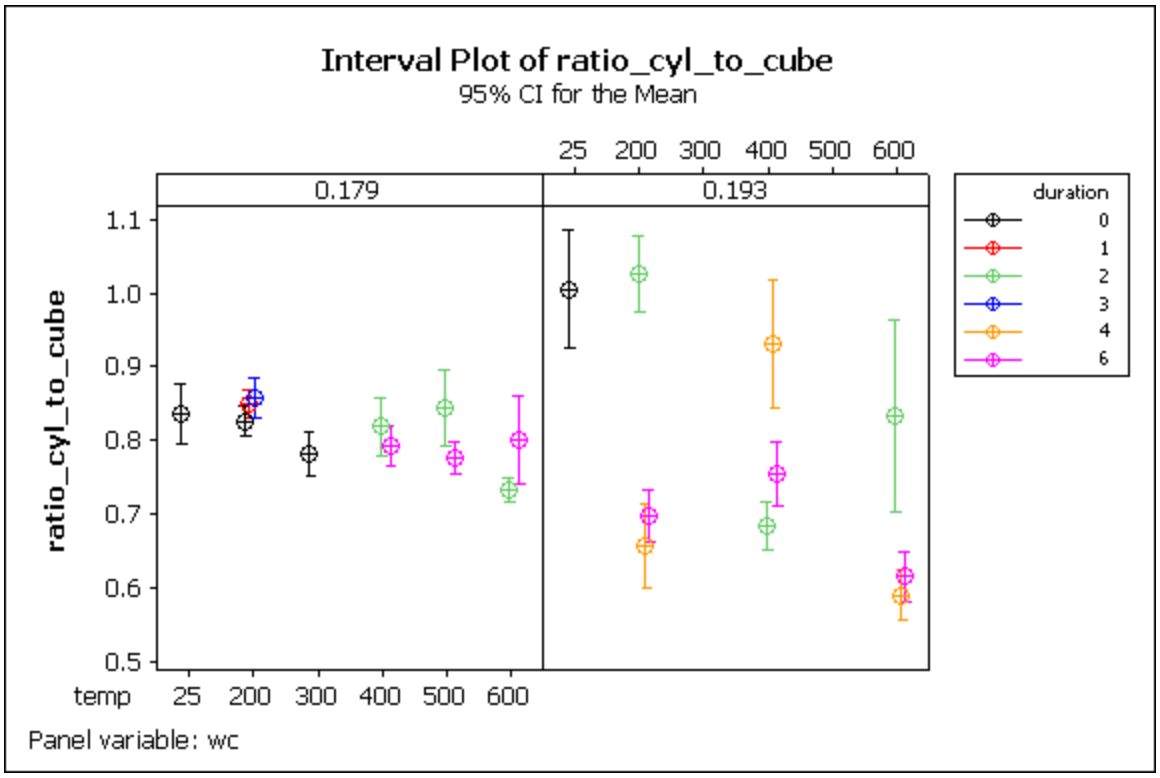


**Fig. 3-13. Interval plot of correlation factor grouped by heating duration and *w/cm* ratio.**

Several attempts have been made to develop a cylinder to cube correlation factor (or conversion factor or coefficient) [14,15,16]. The large number of variables that influence the conversion factor make this a difficult task. These include the size of coarse aggregate, the concrete strength and casting method. It has been observed that the conversion factor approaches 1 as the concretes strength increases [14,17]. In addition to these material properties, the direction of loading with respect to the casting layers (see Fig. 3-14) and the load frame used also influence the correlation factor.

Most of the efforts towards establishing a shape correlation factor focus on normal strength concrete with only a limited number of studies on high-strength concrete. A 2008 study compared the results of compressive strength tests of

100, 70.7 and 51 mm (4, 2.78 and 2 in.) cubes to 102, 76 and 51 mm (4, 3 and 2 in.) cylinders made from UHPC. The authors developed a table of conversion factors for equivalent strengths in either 76 or 102 mm (3 or 4 in.) diameter cylinders (Table 3-10).

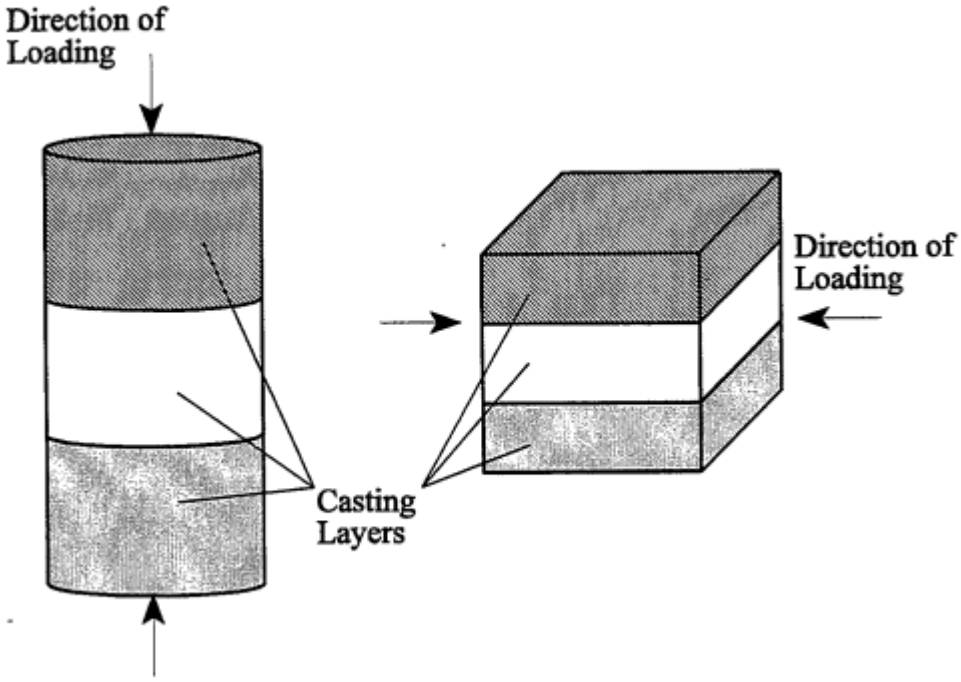


**Figure 3-14. Direction of loading relative to casting direction [18].**

**Table 3-10. Coefficients for conversion of compressive strength results [16].**

| Tested \ Desired | 76 mm diameter cylinder | 102 mm diameter cylinder |
|---|---|---|
| **100 mm cube** | Multiply by 1.00 | Multiply by 1.00 |
| **70.7 mm cube** | Multiply by 0.94 | Multiply by 0.93 |
| **51 mm cube** | Multiply by 0.96 | Multiply by 0.96 |
| **102 mm cylinder** | Multiply by 1.01 | - |
| **76 mm cylinder** | - | Multiply by 0.99 |
| **51 mm cylinder** | Multiply by 1.08 | Multiply by 1.07 |

This table does not provide a conversion coefficient for 51 mm cubes to 51 mm cylinders. However, one can be produced from this table by simple manipulation of the provided ratios. The following conversion coefficients provided in the table:

**(76mm cyl)/(51mm cube) = 0.96 and (76mm cyl)/(51 mm cyl) = 1.08**

From these values, it can be shown that:

**(51mm cyl)/(51mm cube) = (0.96)/(1.08) = 0.889**

The correlation factor and 95% confidence interval of the control specimens from the present experiment is shown in Table 3-11. The derived conversion factor falls within 95% CI all the control specimens and of the higher *w/cm*.

**Table 3-11. Cylinder-Cube Conversion Factor for 51 mm**

| w/cm | Count | Average | Standard Deviation | 95% Confidence Interval | |
|---|---|---|---|---|---|
| | | | | Lower | Upper |
| **0.193** | 15 | 1.006 | 0.145 | 0.861 | 1.079 |
| **0.179** | 16 | 0.836 | 0.077 | 0.759 | 0.873 |
| **Overall** | 31 | 0.918 | 0.142 | 0.776 | 0.968 |

## 3.4 Conclusions

This experiment considered the effects of elevated temperature, exposure duration and specimen geometry on the residual compressive strength of ultra-high performance concrete. In general, the addition of polypropylene fibers proved to be a good mechanism for reducing the explosive spalling of UHPC when exposed to elevated temperatures. The elevated temperatures affected the residual compressive strength of the cylinders and cubes in a similar fashion. The change in residual compressive strength of UHPC with an increase in exposure temperature closely follows that of other concretes. This shows that

UHPC is still vulnerable to the same thermal-mechanical processes that affect all concretes. However, when the exposure duration is considered as a factor the cylinders and cubes respond differently. Durations in excess of one hour had little or no additional effect on residual compressive strength of the cylinders. On the other hand, the exposure duration proved to be a significant factor on the residual strength of the cubes. This apparent duration-specimen geometry effect suggests that the specimen shape is an important factor in the residual strength of UHPC and needs further investigation.

## References


[1] Kosmatka, S. H., Kerkhoff, B., and Panarese, W. C. (2003). *Design and Control of Concrete Mixtures*. EB001, Portland Cement Assoiation, Skokie, IL.

[2] Association Française de Génie Civil, Ultra High Performance Fibre-Reinforced Concretes-Interim Recommendations, Paris, France, 2002.

[3] Graybeal, B. A. (2007). “Compressive Behavior of Ultra-High-Performance Fiber-Reinforced Concrete.” *ACI Materials Journal*, 104(2).

[4] J. Resplendino, J. Petitjean, Ultra-high-performance concrete-First recommendations and examples of application, in: Test and Design Methods for Steel Fibre Reinforced Concrete: Background and Experiences: Proceedings of the RILEM TC 162-TDF Workshop, Bochum, Germany, 20-21 March 2003, RILEM Publications, 2003: p. 91.

[5] P.K. Mehta, P.J. Monteiro, Concrete: microstructure, properties, and materials, McGraw-Hill, 2006.

[6] A.M. Neville, Properties of Concrete., Wiley, New York, 1963.

[7] J.F. Young, S. Mindess, R.J. Gray, A. Bentour, The Science and Technology of Civil Engineering Materials, Prentice Hall, Upper Saddle River, NJ, 1998.

[8] Pimienta, P., and Chanvillard, G. (2004). “Retention of the mechanical performances of Ductal® specimens kept in various aggressive environments.” *FIB Symposium Concrete Structures: Challenge of Creativity, Avignon, France*, 24–28.

[9] Consolazio, G. R., McVay, M. C., and Rish III, J. W. (1998). “Measurement and prediction of pore pressures in saturated cement mortar subjected to radiant heating.” *ACI Materials Journal*, 95(5), 525-536.

[10] Acker, P., and Behloul, M. (2004). “Ductal® Technology: A Large Spectrum of Properties, A Wide Range of Applications.” *Proceedings of the International Symposium on Ultra High Performance Concrete*, 11-24.

[11] R.G. Burg, M.A. Caldarone, G. Detwiler, D.C. Jansen, T.J. Willems, Compression testing of HSC: latest technology, Concrete International. 21 (1999) 67–76.

[12] B.A. Graybeal, Material Property Characterization of Ultra-High Performance Concrete., (2007).

[13] Phan, L. T. (2002). “High-Strength Concrete at High Temperature-An Overview.” International Symposium on Utilization of High-Strength, High-Performance Concrete, June, 16–20.

[14] A.M. Neville, Properties of concrete, J. Wiley, New York, 1996.

[15] J.R. Del Viso, J.R. Carmona, G. Ruiz, Shape and size effects on the compressive strength of high-strength concrete, Cement and Concrete Research. 38 (2008) 386–395.

[16] B.A. Graybeal, M. Davis, Cylinder or cube: strength testing of 80 to 200 MPa (11.6 to 29 ksi) ultra-high-performance fiber-reinforced concrete, ACI Materials Journal. 105 (2008) 603.

[17] J.F. Young, S. Mindess, R.J. Gray, A. Bentour, The Science and Technology of Civil Engineering Materials, Prentice Hall, Upper Saddle River, NJ, 1998.

[18] D.J. Elwell, G. Fu, Compression testing of concrete: cylinders vs. cubes, New York State Department of Transportation, Transportation Research and Development Board, 1995.